Production of High-Grade Mixed Rare Earth Oxides from Acid Mine Drainage via Solvent Extraction: Laboratory-Scale Process Development

Shushu Liu

Thesis submitted to the faculty of

the Virginia Polytechnic Institute and State University

in partial fulfillment of the requirements for the degree of

Master of Science

In

Mining Engineering

Christopher A. Noble, Chair

Emily A. Sarver

Paul F. Ziemkiewicz

December 4th, 2019

Blacksburg, Virginia

Keywords: Rare earth elements, acid mine drainage, solvent extraction

Production of High-Grade Mixed Rare Earth Oxides from Acid Mine Drainage via Solvent Extraction: Laboratory-Scale Process Development

Shushu Liu

ACADEMIC ABSTRACT

Several recent studies have shown that acid mine drainage (AMD) may be a promising source of rare earth elements (REEs), which are essential feedstocks for many high tech applications and defense products. AMD is a longstanding environmental challenge and is currently the primary pollutant of water in the Appalachian coal mining region. Acid generated during the coal mining process tends to leach several transition metals from the surrounding rock strata. While iron, aluminum, and manganese have traditionally been noted as the predominant metals in AMD, recent studies have also shown that REEs are also present, albeit in trace concentrations, often less than 5 μg/L. The recovery of REEs from AMD can be both an economic and environmental advantage; however, the low REE concentrations and high contamination from other metals makes the concentration and purification of REEs quite difficult.

This research seeks to develop and optimize a process capable of producing mixed rare earth concentrates with purities exceeding 90% from an AMD feedstock. Parallel efforts by other members of the research team showed that a solid pre-concentrate, nominally 0.1 to 2% REE, can be readily produced from AMD; however, that pre-concentration process cannot provide the further enrichment needed to generate high purity oxides suitable for downstream markets. In this project, solvent extraction was investigated as secondary process used to further enrich the low grade pre-concentrate to a purity exceeding 90%. Initially, laboratory-scale batch solvent extraction tests were performed on synthetic REE solutions to determine the influence of various process parameters (e.g. pH, extractant dosage, diluent type, and feedstock concentration). Next, the separation of REEs from major AMD gangue elements was investigated using synthetic leachate solutions with concentrations similar to those expected from the pre-concentrate samples. This process showed that the grade targets could easily be met when combining optimal parameters from each step. From this preliminary work with synthetic solutions, an optimal SX process was developed and validated using a real leachate generated from a pre-concentrate sample. By integrating leachate preparation, solvent extraction, scrubbing, stripping, and oxalic acid precipitation, an oxide containing 90.5% rare earth oxides was generated. Details on the process development, experimental optimization, and opportunities for process improvement are described.

Production of High-Grade Mixed Rare Earth Oxides from Acid Mine Drainage via Solvent Extraction: Laboratory-Scale Process Development

Shushu Liu

GENERAL AUDIENCE ABSTRACT

Rare earth elements (REEs) are essential for many modern industries, high-tech applications, and defense products. The U.S. consumes approximately 11% of the global REE demand; however, the US supply chain is heavily reliant on imported Chinese feedstocks. This lack of a domestic supply chain exposes the US to both price and supply volatility, which are prevalent in the international markets. This supply issue is further compounded by a lack of suitable domestic feedstocks. REEs are rarely concentrated into mineable ore deposits, and in some cases the extraction and processing of conventional REEs deposits entails considerable environmental risk. As a result of these challenges, numerous federal agencies and private companies have recently sought to identify promising alternative resources.

One potential alternative resource is acid mine drainage (AMD), which is a common environmental challenge associated with coal and hard rock mining. Prior studies have shown that acid mine drainage contains REEs; however, other metals, such as iron, aluminum, and manganese, preclude REE recovery using conventional processing techniques. As such, the goal of this research is to develop and optimize a process capable of recovering and concentrating REEs from an AMD feedstock.

The research conducted in this thesis predominantly included laboratory testing using synthetic AMD samples. The complexity of the synthetic AMD progressively increased from very simple, single element solutions to complex multi-component mixtures. Through this research, data and information from these controlled experiments was used to design a multi-step solvent extraction process capable of producing final REE products exceeding 90% purity. In the last stage of the research, the final process was validated using actual AMD recovered from an operating mine site. The validation test showed that the process was effective in meeting its initial objectives: the grade of the final rare earth oxide was determined to be 90.5%. This laboratory-scale experimental work represents the first step of process needed to develop and deploy a commercial technology capable of producing REE products from AMD feedstocks.

ACKNOWLEDGMENTS

I would like to express my sincere gratitude to my adviser, Dr. Aaron Noble, for his guidance, motivation, support and patience throughout my entire research work.

This project gave me the opportunity to work with a lot of excellent researchers at both Virginia Tech and WVU. I would like to express my gratitude to all the members of the ETD team.

Next, I would like to thank my committee members, Dr. Paul Ziemkiewicz and Dr. Emily Sarver for their time, advice, and insights.

Special thanks to Jeffery Parks and McAlister Council-Troche for their great help regarding the ICP analysis of all the samples in my research.

I would also like to express my sincere thanks to all my friends and colleagues that I have met in the department during my study in Blacksburg.

At last, I have been so lucky to be brought up by my parents, Yading Liu and Wanxiang Huang, who have always been supportive and considerate of all my decisions. I have also been fortunate to meet my husband, Kaiwu Huang. The love of my parents and husband is the spiritual power that support me to overcome the difficulties in my life.

The financial support from the US Department of Energy is sincerely appreciated. This material is based upon work supported by the U.S. Department of Energy under Award Number DE-FE0026444. This report was prepared as an account of work sponsored by an agency of the United States Government. Neither the US Government nor any agency thereof, nor any of their employees, makes any warranty, express or implied, or assumes any legal liability or responsibility for the accuracy, completeness, or usefulness of any information, apparatus, product, or process disclosed, or represents that its use would not infringe privately owned rights. Reference herein to any specific commercial product, process, or service by trade name, trademark, manufacturer, or otherwise does not necessarily constitute or imply its endorsement, recommendation, or favoring by the US Government or any agency thereof. The views and opinions of authors expressed herein do not necessarily state or reflect those of the US Government or any agency thereof.

TABLE OF CONTENTS

Chapter 1. Introduction 1

1.1 Background on Rare earth elements (REEs) 1

1.1.1 Definition and classification 1

1.1.2 Resource and production 2

1.1.3 Applications of rare earth elements (REEs) 3

1.1.4 Current REEs concerns 4

1.1.5 Alternative sources of rare earth elements (REEs) 4

1.2 Research Aims and Motivation 6

1.2.1 Motivation 6

1.2.2 Research objectives 7

1.2.3 Thesis organization 8

Chapter 2. Literature Review 9

2.1 REEs in Acid Mine Drainage (AMD) 9

2.1.1 REEs in AMD from metal mines 11

2.1.2 REEs in AMD from coal mines 11

2.2 REE Processing Method 13

2.2.1 Conventional REE processing method 13

2.2.2 The process of REE recovery from industrial residue 16

2.2.3 The process of REE recovery from AMD 18

2.3 Solvent Extraction of REEs 20

2.3.1 Basics of solvent extraction 20

2.3.2 Type of extraction system 22

2.4 Summary 26

Chapter 3. Evaluation of Solvent Extraction Operating Parameters using Synthetic REE Solutions 27

3.1. Introduction 27

3.2. Methodology 27

3.2.1 Materials 27

3.2.2 Experimental procedures 29

3.2.3 Extraction Mechanism 30

3.3 Results and Discussion 31

3.3.1 Effect of reaction time 31

3.3.2 Effect of the concentration of REEs in the Feed 32

3.3.3 Effect of D2EHPA concentration, c(D2EHPA) 33

3.3.4 Effect of initial pH in aqueous phase 34

3.3.5 Selection of diluent 35

3.3.6 Selection of stripping reagent 36

3.3.7 Effect of modifier on the solvent extraction system 37

2.4 Conclusions 40

Chapter 4. Development of an REE Solvent Extraction Process using Synthetic AMD Pre-Concentrate Leachate 42

4.1. Introduction 42

4.2 Methodology 42

4.2.1 Materials 42

4.2.2 Experimental procedure 43

4.3 Results and discussion 44

4.3.1 Solvent extraction behavior of elements in simulated leachate 44

4.3.2 Pretreatment of simulated leachate by reduction 47

4.3.3 Stripping behavior of elements in simulated leachate 49

4.3.4 The optimization of phase ratio in scrubbing and stripping stage. 51

4.3.5 Optimal SX process for REE recovery from simulated leachate..... 55

4.4 Conclusions..... 57

Chapter 5. Validation of an Optimal Solvent Extraction Process using Real Leachate derived from AMD Pre-Concentrate 58

5.1 Introduction..... 58

5.2 Methodology..... 58

5.2.1 Materials 58

5.2.2 Chemicals..... 58

5.2.3 Experimental procedure 59

5.3 Results and Discussion 61

5.3.1 The composition of the pregnant leach solution (PLS)..... 61

5.3.2 Fe removal by selectively precipitation 63

5.3.3 SX process 64

5.3.4 Recovery of REE oxalate..... 66

5.3.5 Recovery of REE oxide..... 67

5.3.6 McCabe-Thiele diagrams for extraction and stripping stages 68

4.4 Conclusions..... 69

Chapter 6. Conclusions and Recommendations 71

Reference ……..74

LIST OF FIGURES

Fig 1.1 Rare earth elements in periodic table 1

Fig 1.2 Applications of rare earths elements in United States (after USGS, 2017)..... 3

Fig 1.3 Schematic flowsheet for a process to recover REEs from AMD 8

Fig 2.1 Relationship between pH of raw AMD and the concentration of TREE (Vass, 2019) 10

Fig 2.2 A flowsheet of conventional REE extraction and refining flowsheet 14

Fig 2.3 The average distribution of major elements in 141 AMDp samples (Vass, 2019) 19

Fig 2.4 schematic of solvent extraction process (after Gupta and Krishnamurthy, 1992) 21

Fig 3.1 Yamato SA320 horizontal-vertical laboratory shaker 30

Fig 3.2 Effect of reaction time on the extraction efficiency of Y(III) 32

Fig 3.3 Effect of feed concentration on the extraction efficiency of Dy(III)..... 33

Fig 3.4 Effect of D2EHPA concentration on the extraction efficiency of REEs..... 34

Fig 3.5 Effect of initial on the extraction efficiency of REEs. 35

Fig 3.6 Comparison between Kerosene and Elixore Range of the extraction efficiency of REEs. 36

Fig 3.7 Effect of acid concentration on the stripping efficiency..... 37

Fig 3.8 Stripping Solution (a) Without TBPO (b) With TBPO 38

Fig 3.9 Effect of pH on the extraction efficiency of Sc(III), Ce(IV), Nd(III), Dy(III) and Y(III) at different TBPO concentrations..... 39

Fig 3.10 pH-extraction isotherms of Ce(IV), Nd(III), Dy(III), Y(III) and Sc(III) at different TBPO concentrations 40

Fig 4.1 Extraction behavior of major elements and REEs in simulated leachate. 46

Fig 4.2 The effect of reaction time on the reduction efficiency of Fe 48

Fig 4.3 The effect of reductant dosage on the extraction efficiency of Fe 49

Fig 4.4 Stripping behavior of major elements and REEs in simulated leachate. 50

Fig 4.5 The preliminary SX process for the recovery of REEs from simulated leachate. 51

Fig 4.6 The effect of phase ratio on the scrubbing efficiency of gangue metals 52

Fig 4.7 The effect of phase ratio on the scrubbing efficiency of REEs 53

Fig 4.8 The effect of phase ratio on the stripping efficiency 54

Fig 4.9 The effect of phase ratio on elemental composition of strip liquor 54

Fig 4.10 The flowsheet and elemental composition of each stream of the optimized SX process 56

Fig 4.11 Compositions of REO product generated from simulated leachate 57

Fig 5.1 The photo of pregnant leach solution (a) and leachate (b) 60

Fig 5.2 Recovery of REEs and gangue metals in selectively precipitation 63

Fig 5.3 Concentration of the elements in the product of each stage in SX process 65

Fig 5.4 Recovery of REEs and in precipitation by oxalic acid 67

Fig 5.5 McCabe-Thiele diagram of extraction of TREE from leachate 68

Fig 5.6 McCabe-Thiele diagram of stripping of TREE from loaded organic 69

Fig 5.7 Flowsheet of the recovery of MREO from pre-concentrate of AMD 70

LIST OF TABLES

Table 1.1 Global rare earth mine production and reserves (after USGS, 2019) 2

Table 2.1 The total REE concentration in AMD from metal mine in different regions ... 11

Table 2.2 TREE for AMD and AMDp from nine coal mine sites (Vass et al., 2019)..... 13

Table 2.3 The solution obtained from acid leaching of three AMDp samples (Vass, 2019) 20

Table 2.4 Some commercial extractants for rare earth solvent extraction..... 23

Table 3.1 Concentrations of REE in the feed solutions. 27

Table 3.2 Technical Data for Elixore Diluents (after Elixore, 2014) and Kerosene (Wikipedia) 35

Table 3.3 The distribution of Sc(III) in the stripping process..... 38

Table 4.1 The target and actual concentrations of elements in simulated leachate 43

Table 4.2 Extraction efficiency of elements in simulated leachate 45

Table 4.3 The results of solvent extraction test with 2.5 vol.% TBPO at phase ratio (V_O/V_A) of 1:3 47

Table 4.4 The concentrations of elements in the loaded organic phase..... 49

Table 4.5 The concentrations of elements in the organic feed for the stripping stage 53

Table 4.6 Comparison of the elemental composition of simulated leachate (SL) and strip liquor 55

Table 5.1 Element composition of the dry REE concentrate..... 59

Table 5.2 Elemental composition of the PLS 62

Table 5.3 Elemental composition of the leachate 64

Table 5.4 Concentration of the elements in the product of each stage in SX process 66

Table 5.5 Compositions of REO product from pre-concentrate of AMD 67

ABBREVIATION

AMD	Acid Mine Drainage
AMDp	Acid Mine Drainage Precipitate
D2EHPA	Di-2-ethyl-hexyl-phosphoric acid
HREE	Heavy Rare Earth
ICP-MS	Inductively Coupled Plasma Mass Spectrometry
LREE	Light Rare Earth
MREO	Mixed Rare Earth Oxide
PLS	Pregnant Leach Solution
REEs	Rare Earth Elements
REO	Rare Earth Oxide
SX	Solvent Extraction
TBPO	Tri-butyl phosphine Oxide
TREE	Total Rare Earth Elements
TMM	Total Major Metals

Chapter 1. Introduction

1.1 Background on Rare earth elements (REEs)

1.1.1 Definition and classification

Rare earth elements (REEs) are a group of 17 elements including the 15 lanthanides, scandium, and yttrium, which is highlighted in Figure 1.1. Scandium (Sc) and Yttrium (Y) are considered as REEs because of their similarity in chemical and physical properties, as well as their co-occurrence in nature. Normally, the lanthanides can be classified into two groups, the light rare earth elements (LREEs) –lanthanum (La) to europium (Eu), and the heavy rare earth elements (HREEs) –gadolinium (Gd) to lutetium (Lu), based on their geochemical properties (Jordens, Cheng, & Waters, 2013). Yttrium (Y) is usually classified into HREEs and placed between Dysprosium (Dy) and Holmium (Ho) due to their similar chemical properties (Bau, 1996). Scandium is commonly grouped in neither the HREEs nor LREEs due to its much smaller ionic radius, and therefore this element is treated separately (Jha et al., 2016). REEs can also be classified as critical (Y, Nd, Eu, Tb, Dy), uncritical (La, Pr, Sm, Gd) and excessive (Ce, Ho, Tm, Yb, Lu) based on the forecasts on both demand and supply of every REE in recent years (Seredin & Dai, 2012).

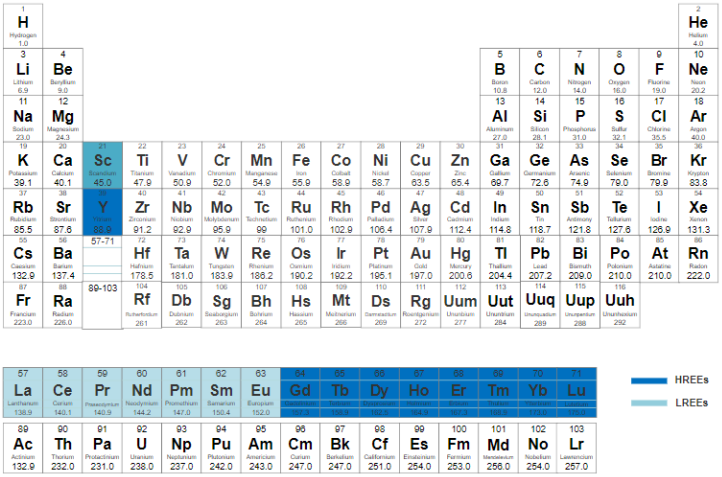

Fig 1.1 Rare earth elements in periodic table

1.1.2 Resource and production

Despite the name “rare earth”, these metals are not as “rare” as their name shows. The concentration of REEs in Earth’s crust is estimated to between 150 to 220 parts per million, which is higher than the concentration of many common metals for industrial use, such as Cu or Zn (Long et al., 2012). Even Lutetium (Lu) and thulium (Tm), which are the least abundant among the REEs, are much more abundant than gold in Earth’s crust (Walawalkar, 2016).

Table 1.1 Global production and reserves of rare earth (after USGS, 2019)

(Data in metric tons of rare earth oxides(REO) equivalent content)

	Production /tons		
Country	2017	2018	Reserves/tons
United states	-	15,000	1,400,000
Australia	19,000	20,000	3,400,000
Brazil	1,700	1,000	22,000,000
Burma	NA	5,000	NA
Burundi	-	1000	NA
China	105,000	120,000	44,000,000
India	1,800	1,800	6,900,000
Malaysia	180	200	30,000
Russia	2,600	2,600	12,000,000
Thailand	1,300	1,000	NA
Vietnam	200	400	22,000,000
Other countries	-	-	4,400,000
World total(rounded)	132,000	170,000	120,000,000

There are a wide variety of minerals containing rare earths, but the primary REEs-bearing minerals are bastnaesite, xenotime, monazite, apatite, ioparite and ion-absorption clays (Jordens et al., 2013). Among them, 95% REEs are produced from monazite, xenotime, and bastnasite (Walawalkar, 2016). In these minerals, rare earths commonly occur as oxides, carbonates, phosphates and silicates, of which 60% of rare earths exist as oxide (Krishnamurthy & Gupta, 2004). China and Brazil have the two largest reserves of

rare earths in the world. China is also the largest producer of rare earths and contributes to more than 90% of the world rare earth production since 1980s (Chakhmouradian & Wall, 2012). The global rare earth reserves and production are listed in Table 1.1.

More than 250 minerals have been recognized as rare earth minerals, but most of them cannot be refined in an economic manner as the concentration of REEs is very low varying from 10 to 300 ppm (J Zhang & Edwards, 2012). Furthermore, REEs are interchangeable in most minerals due to their similar ionic radii, which makes it very difficult to separate them to obtain high purity rare-earth product (Jordens et al., 2013).

1.1.3 Applications of rare earth elements (REEs)

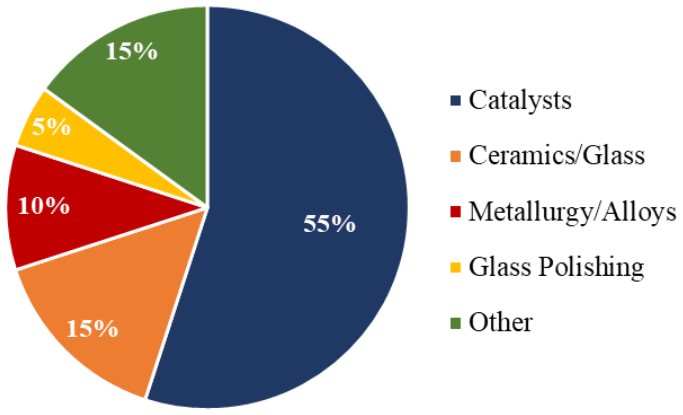

Fig 1.2 Applications of rare earths elements in United States (after USGS, 2017)

Due to their unique chemical, magnetic, electrical, and catalytic properties, REEs are widely used in many fields, such as nuclear, magnets, electronics, and catalysts (Massari & Ruberti, 2013). The applications of REEs can be divided into two areas. One is the traditional area including petroleum and chemical industry, glass and ceramics, metallurgy and machinery. In this area, REEs are always used in the forms of mixed rare earth metals and alloys. The other one is the high-tech area. REEs has been integrated into every part of modern life. Many high-tech products depend on REEs, especially in the field of electronics and renewable energy, like televisions, cell phones, computers, LED light lamps, hybrid cars, wind turbines, and so on. REEs are used in the form of high purity single rare earth oxide (Jack Zhang, Zhao, & Schreiner, 2016). Figure 1.2 shows the applications of REEs in United States.

1.1.4 Current REEs concerns

With the rapid development of industries mentioned above, the global demand for rare earth is projected to grow at an annual rate of 5% by 2020 (Dutta, et al., 2016). Therefore, it is expected that there will be a supply crisis of some REEs in the next 15 years (Al-Thyabat & Zhang, 2015). However, due to the increasing domestic demands, China drastically reduced the exports of rare earth raw materials by 40% in 2010, which made the rare earth prices shoot up to 1500% just a few months (Hatch, 2012). As a result, other countries initiated research projects to identify alternative REEs sources and develop their own REEs supply chain, especially for the countries that depend on Chinese exports. For example, the United States has formulated a strategy to address the challenges in current global REEs market. Three approaches are put forward to proactively address REEs supply risks and prevent supply chain disruptions, which are: (1) achieve globally diverse supplies; (2) identify appropriate substitutes; (3) improve the capacity for recycling, reuse and more efficiency use of critical materials (Chu, 2011).

1.1.5 Alternative sources of rare earth elements (REEs)

(1) Rare-earth deposits

The supply risk of REEs sets in motion a search for new REEs deposits and the re-opening of old rare earth mines. The production of REEs often comes with serious environmental issues including the release of radioactive tailings and the damage of the ecosystem. Mountain Pass mine, the only rare earth mining and processing facility in the United States, closed in 2002 in response to environmental restriction. However, it has been reopened to ease the supply crisis.

(2) Urban mining of end-of-life products

Urban mining is one of the most creative solutions to obtain REEs without inducing additional environmental problems. Urban mining is simply defined as the process of reclaiming raw materials from spent products, buildings and waste. Urban mining is applied to mitigate REEs supply crisis by reclaiming REEs from end-of-life products. This method is focusing on the resources with high concentration of REEs, such as phosphor-containing products, permanent magnets and NiMH batteries, but the

total available amount for recycle is relatively low (Binnemans et al., 2015; Binnemans & Jones, 2014; Sprecher et al., 2014).

Yang et al. studied the recovery of REEs from the phosphor powder in waste fluorescent lamps by acid leaching and solvent extraction (Yang, Kubota, Baba, Kamiya, & Goto, 2013). A study on the extraction of REEs from the Nd-Fe-B magnet scraps indicated that the 90% of Neodymium (Nd) was recovered by using NH_4Cl as the chlorination reagent (Itoh, Miura, & Machida, 2009). Pietrelli et al. developed a hydrometallurgical process for recovery of metals from spent NiMH batteries and 80% of REEs were recovered by precipitation of sodium REE double sulfate (Pietrelli et al., 2002). However, according to the report on recycling rate of metals, less than 1% of the REEs was recycled in 2011 (Graedel et al., 2011).

(3) Rare-earth-containing industrial residues

Compared with the urban mining of the end-of-life products, much less attention has been paid to rare-earth-containing industrial residues, like bauxite residue (red mud), phosphoric acid by product, and waste water. Generally, these resources contain much lower concentration of REEs than end-of-life products, but their total reserves are significantly larger.

Phosphogypsum and phosphoric acid sludge are the main by-products in the production of phosphoric acid (Koopman & Witkamp, 2000). Phosphate rock contains REEs with the concentration between 0.01 and 0.1 wt%, and cerium, lanthanum and neodymium account for 80% of total REEs. During the production of phosphoric acid, 70% to 85% of the REEs ends up in the phosphogypsum (Habashi, 1985) and 15% to 30% of REEs report to the phosphoric acid (Wu et al., 2018). The obtained phosphoric acid is evaporated to achieve commercial grade where REEs are precipitated in the sludge. Among the phosphate mining and processing streams, the sludge contains the highest concentration of REEs over 2000 mg/L (Allaedini & Zhang, 2019).

Waste water is also a potential resource of rare earth. Acid mine drainage (AMD) contains considerable concentrations of rare earths (Zhao et al., 2007). AMD is the outflow of acidic water from metal mines or coal mines (Akcil & Koldas, 2006). It is metal-rich water from chemical reaction between water and rock materials containing

sulfur-bearing minerals. The behavior of heavy metals in AMD has been thoroughly investigated (C. A. Johnson, 1986; Schemel, Kimball, & Bencala, 2000; Ali, 2014). However, less research is focused on REEs and the potential of AMD as REEs feedstock is largely unexplored.

1.2 Research Aims and Motivation

1.2.1 Motivation

In response to the global supply crisis of REEs and the dominance of China, the development of domestic supply chain has become a necessity for the United States. Reopening the REE deposits can be a solution, however, the REE deposit are extremely uncommon in U.S. and the rare earth mining and extraction procedures will cause massive environmental problems including the release of radioactive tailings and the damage of the ecosystem. People turn their attention to the recycling of REE from end-of-life products. However, the overall recyclable volume is relatively small to the increasing worldwide demand for REEs. It may help mitigate the supply crisis but not likely to contribute significantly to the rapidly growing REE demand. In this case, people seek to identify the alternative REE resource to compensate for the gap between the supply and demand over the next several years.

Recent studies at West Virginia University (WVU) and Virginia Tech (VT) have shown that the acid mine drainage (AMD) is enriched in REEs. The REE concentrations in the precipitates (AMDp) formed during AMD treatment are even higher than many of the best commercial deposits worldwide. Besides, unlike the conventional rare earth deposits where REEs are encased in ores, the REEs in AMD are already liberated from the host rock. It is more efficient to recover REEs from AMD than the hard-rock deposits (Ziemkiewicz, 2016). Moreover, the total reserves of AMD are significant. Researchers at WVU evaluated the REE reserves at hundreds of AMD treatment sites. It is estimated that more than 800 tons of REEs can be generated per year only in the area of Pennsylvania and West Virginia (Vass et al., 2019).

Therefore, the U.S. Department of Energy - National Energy Technology Laboratory has identified the AMD as a potentially promising source of REEs. The

project (DE-FE0026444) brings together the researchers in universities and industry to collaborate on developing a process to generate commercial REE products from AMD. If successful, the project will not only contribute to the domestic REE supply chain but also bring new opportunities for the development of Appalachia's coal industry.

1.2.2 Research objectives

The researchers in WVU identified and characterized the occurrence of REEs in AMD and AMDp generated by coal mining in Appalachian basins. It has been shown that AMDp contains elevated concentrations of REEs. Therefore, a processing route was developed to extract REEs from AMDp (Vass, 2019). However, this method excludes the REEs in the raw AMD resource which contains a much larger amount of total REEs than AMDp. Therefore, an alternative process of REE recovery was developed to treat raw AMD instead of AMDp. A simplified flowsheet of the process is provided (Fig 1.3). In this process, the raw AMD is processed to create high quality precipitate, which is called pre-concentrate. The process then follows a hydrometallurgical processing route. The REE in the pre-concentrate is first extracted into the solution with acid leaching, and the resulted leach solution is purified and concentrated by solvent extraction (SX). Then the oxalic acid can be used to precipitate REEs in aqueous phase to generate a mixed REE concentrate with >90% purity by mass. Finally, the refining process is used to produce individual REE product.

The main objective of this study is to develop a laboratory-scale solvent extraction process to recover high purity mixed REE oxide (MREO) from AMD pre-concentrate. Three specific objectives were as follows:

1) Investigate the parameters influencing the solvent extraction to determine the optimal chemical conditions for the recovery of REEs.
2) Investigate the separation of REEs from the gangue metals and determine an optimal solvent extraction process to recover high purity MREO.
3) Develop a processing flowsheet to generate MREO that exceeds 90% purity from AMD pre-concentrate.

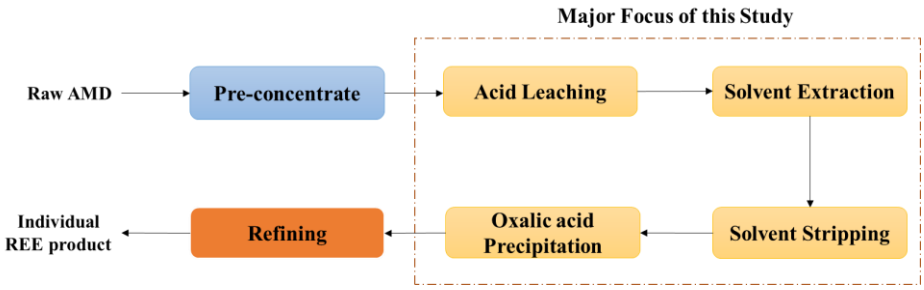

Fig 1.3 Schematic flowsheet for a process to recover REEs from AMD

1.2.3 Thesis organization

This thesis is organized into six chapters. **Chapter 1** is an introduction of the background, research aims and motivation. **Chapter 2** reviews the literature regarding the REE in the AMD, REE processing methods of conventional and unconventional resources as well as the solvent extraction of REEs.

Chapter 3 investigates the recovery and transport of REEs in the solvent extraction system. In this chapter, an artificial solution containing five surrogate REEs is used to investigate the effects of parameters on the recovery of REEs, and to determine the optimal experimental conditions for the extraction of REEs. The results are used for the development of the processing route to separate REEs from the gangue metals in **Chapter 4**.

Chapter 4 investigates the separation of REEs from the gangue metals. The extraction tests were firstly performed with a simulated leachate with five surrogate REEs and gangue metals. The elemental composition of the simulated leachate was designed similar to that of an actual AMD pre-concentrate. The latter was obtained by a preliminary pre-concentrate process developed by Ziemkiewicz's group in WVU. An optimal solvent extraction process has been developed to recover high purity MREO from the simulated leachate.

Based on the optimal solvent extraction process derived from **Chapter 4**, **Chapter 5** develops a processing flowsheet to generated high purity MREO from a AMD pre-concentrate with 0.1% REE.

The conclusions in this thesis are summarized in **Chapter 6**. In this chapter, the recommendations are also presented.

Chapter 2. Literature Review

2.1 REEs in Acid Mine Drainage (AMD)

The production of acidic metal-rich effluents, which is usually referred to as acid mine drainage (AMD), has been described as one of the largest environmental problems caused by mining activities (Akcil & Koldas, 2006). AMD mostly occurs when mining or mineral processing is done to extract from the sulfide-bearing minerals, such as metal mines containing pyrite (FeS), chalcopyrite (Cu_2S), pyrrhotite ($Fe_{1-x}S$), sphalerite (ZnS) and galena (PbS) (Akabzaa, Armah, & Baneong-Yakubo, 2007; Chapman, Jones, & Jung, 1983; Jung et al., 2005) and coal deposits containing pyritic-sulfur and organic sulfur (Brake, Connors, & Romberger, 2001; Foos, 1997).

When sulfide minerals are exposed to air and water, the oxidation and hydrolysis reactions of sulfides produces sulfuric acid and leaches out heavy metals to the drainage (Blowes et al., 2003; Brake et al., 2001). Pyrite and marcasite (both forms of FeS_2) are predominant sulfides in coal regions (Skousen & Ziemkiewicz, 1996). Reaction 2.1 shows the oxidation process of the FeS_2.

$$2FeS_2 + 7O_2 + 2H_2O \rightarrow 2Fe^{2+} + 4SO_4^{2-} + 4H^+ \qquad 2.1$$

Here, the sulfur is oxidized to form hydrogen ions and sulfate, which are components required for sulfuric acid. The soluble Fe^{2+} is left in the solution and free to react further.

$$4Fe^{2+} + O_2 + 4H^+ \rightarrow 4Fe^{3+} + H_2O \qquad 2.2$$

In Reaction 2.2, the Fe^{2+} is oxidized to Fe^{3+} slowly at low pH values (USEPA, 1994).

Additionally, the presence of bacteria will allow the FeS_2 to be dissolved when it is in contact with Fe^{3+}, which is described in Reaction 2.3 (USEPA, 1994).

$$FeS_2 + 14Fe^{3+} + 8H_2O \rightarrow 15Fe^{2+} + 2SO_4^{2-} + 16H^+ \qquad 2.3$$

Finally, the hydrolysis of Fe^{3+} happens and generates $Fe(OH)_3$ as shown in Equation 2.4, which composes the orange solids commonly seen in the AMD impacted area (USEPA, 1994).

$$Fe^{3+} + 3H_2O \rightarrow Fe(OH)_3 + 3H^+ \qquad 2.4$$

The sulfuric acid produced from oxidation tends to mobilize the metals from shale. The acidity of water will further increase as these metals undergo hydrolysis reaction (Hedin, 2006). Therefore, AMD is generally characterized by low pH value and high concentrations of metal ions like Fe, Al, Ca, Mn, Mg, Zn, Ni and so-on, which exceeds the standards of the local surface water quality (Brake et al., 2001).

REEs are often found enriched in the AMD-impacted regions. Studies on the REE mobility in water as well as in the leaching tests of soils shows a strong relationship between low pH and high REE concentrations (Noack, Dzombak, & Karamalidis, 2014). In addition, the dissolved REEs react with SO_4^{2-} by the formation of $(RE)SO_4^+$, which is the primary form of dissolved REE (Grawunder, Merten, & Büchel, 2014; Zhao et al., 2007). The rare earth sulfate complexes ($(RE)SO_4^+$) are also likely absorbed onto the Fe–Al–Mn oxide/hydroxide colloids forming co-precipitates, or precipitating directly as $RE(OH)_3$, thereby, resulting in the decrease of REE concentrations with the increase of pH (Zhao et al., 2007). Figure 2.1 shows the relationship between the concentration of total REEs (TREE) and the pH of AMD collected from Central and Northern Appalachia (Vass, 2019). The data also shows that lower pH correlates with higher REE concentrations.

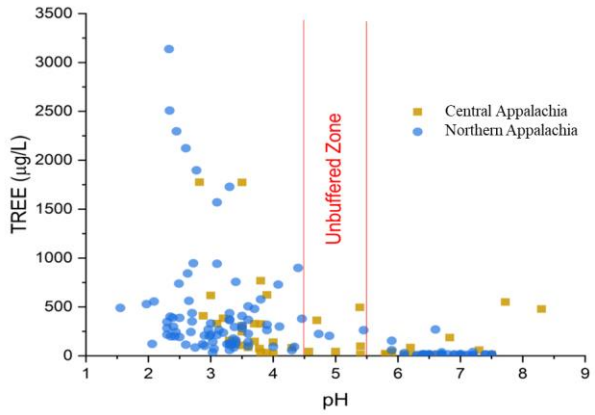

Fig 2.1 Relationship between pH of raw AMD and the concentration of TREE (Vass, 2019)

2.1.1 REEs in AMD from metal mines

The REE concentration in AMD varies in different regions depending on the physicochemical characteristics of the source rock and local conditions (Table 2.2). A total REE concentration of 29 mg/L was measured by researchers in near surface water impacted by AMD from Osamu Utsumi uranium mine in Brazil (Miekeley et al., 1992). In Romania, a total REE concentration of 1.6 mg/L were detected in the ground water from a deposit which was rich in Cu, Zn, Pb and Ag (Grawunder et al., 2014). In Urumieh-Dokhtar magmatic belt, which is known for Cu-bearing region in Iran, a total REE concentration of up to 0.4 mg/L was reported in the AMD from one of the coper mines, which was much higher than the natural water (0.83 ug/L to 1.71 ug/L) (Soltani, Moore, Keshavarzi, & Sharifi, 2014). For a copper mine in Portugal, the AMD contains an average REE concentration of 0.2 mg/L (Pérez-López et al., 2010). For pyrite mine areas in Portugal, the REE concentration in AMD ranges from 0.3 mg/L to 2.8 mg/L (Da Silva et al., 2009).

Table 2.1 The total REE concentration in AMD from metal mine in different regions

TREE, mg/L	pH	Location	Reference
29	3.6	Osamu Utsumi Uranium Mine, Brazil	(Miekeley et al., 1992)
1.6	3.6	Hanes, Romania	(Grawunder et al., 2014)
0.5	2.5	Sarcheshmeh copper mine, Iran	(Soltani et al., 2014)
0.2	2.3	Sao Domingos copper mine, Portugal	(Pérez-López et al., 2010)
1.9-3.0	0.3-2.8	Lousal mine area in Iberian Pyrite Belt, Portugal	(Da Silva et al., 2009)

2.1.2 REEs in AMD from coal mines

Pyrite is generally abundant in the coal layer and both coal and host rock (McCarthy, 2011). Coal is extracted either by underground mining or by opencast methods. When the coal mine is in production underground, the water table is kept low by pumping. However, when the pumps are turned off after the production terminates, the surrounding groundwater fills in the mine void and becomes acidified by reacting with

sulfide minerals, finally leading to the AMD discharged (D. B. Johnson & Hallberg, 2005). Rock blasting is commonly used in opencast mining process. After production, the broken rock is then backfilled and covered by soil. When the water flows through the mine region, it reacts with the pyrite liberated from backfill materials resulting in lowered pH and the release of high concentration of metals (McCarthy, 2011). The AMD discharge starts when mining is initiated and causes lasting damage to local water.

AMD from coal mine also contains high concentration of REEs. Although a lot of work has been conducted on the REE characterization of AMD from metal mines, less research related to coal mines is reported (Sahoo et al., 2012). For Jaintia Hills coalfield in India, the total REE concentration of AMD on average is up to 717.7 ug/L (Sahoo et al., 2012). In China, an average REE concentration of 61.21 ug/L in AMD was reported from Sitai coal mine of Shanxi Province (Zhao et al., 2007). Another research on the nearby coal area shows the concentration of total REE in AMD decreased from 520 to 0.875 ug/L as the pH increased from 4 to 6 (H. Sun et al., 2012). Compared to some metal mines, there is lower concentration of REEs in the AMD generated from coal mines. However, the total reserves of AMD from coal mines are tremendous.

Stewart et al. investigated the distribution of metal elements in AMD collected from a variety of mine water from Appalachian Basin coal belt. It was shown that the most of AMD discharges were enriched with rare earth elements, which was 1-4 orders of magnitude compared to ground waters and uninfluenced surface. The AMD in Appalachian Basin was estimated to generate a total of about 538 metric tons of REEs per year in a dissolved state. Therefore, the AMD from coal mines represent a new potential source of REEs in the U.S (Stewart et al., 2017).

The mines are required to treat AMD before it can be discharged into the environment by removing metals like Fe, Al, Mg and bringing pH to neutral to ease the ecological pollution. The treatment of AMD often involves the neutralization with lime or limestone and follows by precipitation. It is found that the REEs are concentrated in the precipitated sludge (AMDp) but not in the water discharged to the stream (Ziemkiewicz et al., 2016). The analysis of AMDp by different AMD treatment including Fe oxy-hydroxides, Ca-Mg lime slurries, and Si- and Al-rich precipitates also indicates

that the precipitated sludge is enriched in REEs relative to the average AMD value by factors of about 100 (Stewart et al., 2017). In other words, the treatment of AMD is a kind of concentration of REEs. Vass et al. compares the total concentration of REEs (TREE) in AMD and AMDp in nine Northern Appalachian coal mine sites. Among the tested samples, the average of TREE in AMD was 0.258 mg/L while that in AMDp was up to 517 g/ton with a concentration factor of 2000 times (Vass, Noble, & Ziemkiewicz, 2019).

Table 2.2 TREE for AMD and AMDp from nine coal mine sites (Vass et al., 2019)

Site ID	Influent pH	Treatment chemical	TREE in AMD, mg/L	TREE in AMDp, g/ton
1	2.73	Lime	0.116	710
2	6.91	Lime	0.008	641
3	3.46	NaOH	0.153	422
4	3.17	Lime	1.139	664
5	2.88	Lime	0.314	1286
6	5.38	Lime	0.057	711
7	6.58	Lime	0.030	152
8	2.69	Lime	0.182	40
9	2.70	Lime	0.321	29
Mean	-	-	0.258	517

2.2 REE Processing Method

2.2.1 Conventional REE processing method

The recycling of REE is currently very limited and based on conventional methods used to produce REE from minerals. The technological scheme of extracting REE from minerals commonly consists of crushing and milling ores, physical beneficiation to produce REE concentrate, the chemical extraction and further purification and separation to generate REE oxides (Krishnamurthy & Gupta, 2004). Figure 2.2 shows a simplified flowsheet from mine ore to REE oxides product (Zaimes et al., 2015).

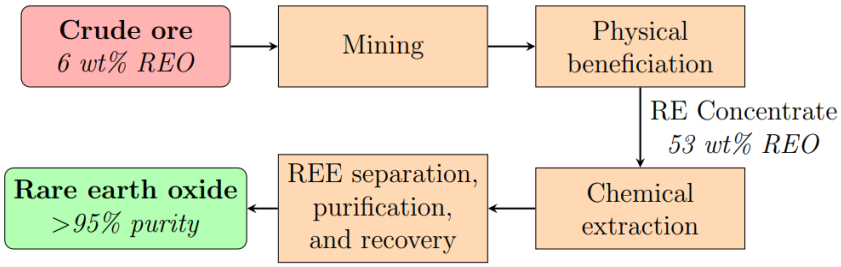

Fig 2.2 A flowsheet of conventional REE extraction and refining flowsheet

The primary REE bearing minerals that have been extracted on a commercial scale are bastnasite ($RECO_3F$) and monazite ($REPO_4$). Next to these, ion-absorbed clays are more and more important as a primary resource as their unique REE distribution (Peelman et al., 2016). The primary separation processes used in the beneficiation of these minerals are gravity concentration, magnetic separation, electrostatic separation, and froth flotation (Krishnamurthy & Gupta, 2004).

The rare earth minerals have relatively high specific gravities which are between 4 and 7, while the primary associated gangue minerals like quartz have much lower density (Ferron, Bulatovic, & Salter, 1991). Therefore, gravity separation can be used to concentrate rare earth minerals. Magnetic separation is commonly utilized in the beneficiation of REE to eliminate minerals with highly magnetism. Besides, some REE minerals like monazite and xenotime have a certain degree magnetism because the electrons in the shielded 4f sub-shell of REE have magnetic moments that do not cancel out. As a result, these REE minerals can be beneficiated through magnetic separation (Krishnamurthy & Gupta, 2004). Electrostatic separation is achieved by using the difference in the conductivity of mineral particles (Kelly & Spottiswood, 1989). This technology is basically only used when other methods are not effective because it is required to drive off all moisture in materials before electrostatic separation. The energy requirement will be significant for the ores that need wet comminution before beneficiation. Compared to the other beneficiation methods, much more research has been conducted on the froth flotation of REE minerals (Krishnamurthy & Gupta, 2004). The flotation is popular due to its capacity and adaptability. It is able to process fine particles with a wide range of sizes and can be tailored to a given deposit with unique mineralogy (Jordens et al., 2013).

Following the physical beneficiation, hydrometallurgical processing methods are applied to the purification and separation of REEs, which includes chemical leaching, selective oxidation, selective reduction, fractional crystallization, fractional precipitation, ion exchange and solvent extraction (Krishnamurthy & Gupta, 2004).

Chemical leaching is used to extract REEs from solid REE concentrate. Common processes include acid and alkaline leaching for primary ores and leaching with NaCl or $(NH_4)_2SO_4$ for ion-absorbed clays. The leaching reagent is selected according to the characteristic of minerals, subsequent separation processing and targeted REE product (e.g. chlorides vs. oxides) (Noack, 2015). For bastnaesite, the first step of leaching process is to decompose the fluorocarbonate matrix (REF_3-$RE_2(CO_3)_3$) with H_2SO_4, and then the fluoride (REF_3) is decomposed by NaOH at high temperature. The REEs are converted to leachate or hydroxides for subsequent process. The acid leaching is currently used at Bayan Obo mine in China and the alkaline leaching was used at the Mountain Pass mine (Krishnamurthy & Gupta, 2004). For monazite, the REE hydroxides is dissolved in a hot acidic solution after alkaline treatment. The selection of acid is based on the subsequent solvent extraction process. For example, HNO_3 will be used for solvent extraction with tri-butyl phosphate and H_2SO_4 will be selected for solvent extraction with amines (Peelman et al., 2016). HCl leaching or roasting with chlorine are also developed for the production of rare earth chlorides from bastnasite and monazite (Hartley, 1952).

The solution obtained from the leaching process is a mixture of REEs with other metals. Purification and separation processes are followed to produce final rare earth products. Many of the final products are mixed REE materials, such as mischmetal and mixed rare earth oxides (Krishnamurthy & Gupta, 2004). These materials can be further purified to generate high purity products. The separation of individual REE can be achieved by various ways, e.g., selective oxidation, selective reduction, fractional crystallization, fractional precipitation, ion exchange and solvent extraction, which are all based on the difference in basicity (Krishnamurthy & Gupta, 2004). Among these methods, solvent extraction and ion exchange have been developed thoroughly to produce high purity rare earth products. However, compared to ion exchange, solvent extraction is capable of handling a large volume of rare earth solution with high concentrations, which makes the process very compact. Solvent extraction is also a

flexible method, which can produce rare earth products at required purities (Stewart et al., 2017; Jack Zhang et al., 2016). As a result, solvent extraction is currently viewed as the most applicable method for the purification and separation of REEs.

2.2.2 The process of REE recovery from industrial residue

Some studies report on the recovery process of Fe and Al from AMD sludge by selective precipitation (Wei, Viadero Jr, & Buzby, 2005). However, limited information is available on the recovery process of REEs. Fortunately, many studies have been conducted on the REEs recovery from the sludge or waste residue generated during other industrial production, such as the phosphogypsum and phosphoric acid sludge produced during phosphoric acid production (H. Li, 2010) and red mud produced from alumina production (Borra, Blanpain, Pontikes, Binnemans, & Van Gerven, 2016). All of these materials are similar to AMD as they are all with complex mineral phases and contain high concentrations of impurity elements like Al, Ca, Fe with relative low REEs content (Liu & Naidu, 2014). As such, a review of the efforts on recovering REE from these industrial residue is critical to explore the recovery process of REEs from AMD.

Apatite is the main resource for phosphorous in phosphoric acid industry which contains 0.1%-1% REE (Habashi, 1985). Phosphoric acid is produced by a wet-process, in which the apatite is digested with sulfuric acid and a mixture of phosphogypsum and phosphoric acid generate. During the production of phosphoric acid, 70% to 85% of the REEs ends up in the phosphogypsum (Habashi, 1985). The recovery of REE from phosphogypsum has been investigated for several decades. The recovery processes generally include leaching of REEs with sulfuric acid, nitric acid or hydrochloric acid and extraction of REEs by the methods of precipitation, solvent extraction, ion exchange as well as crystallization (Podbiera-Matysik, Gorazda, & Wzorek, 2015).

The leaching of phosphogypsum is able to obtain a high recovery of REEs. However, the concentration of REEs is very low in the leachate. At this time, precipitation method is commonly employed because the REEs can precipitate as hydroxides, oxalates or double sodium-REE sulfates even at low concentration (Podbiera-Matysik et al., 2015). A process of REE recovery from phosphogypsum with two-step precipitation was reported in 1980s in Poland. The REE in the leachate firstly

precipitated as double sulfates with a mixture of NaOH and Na_2SO_4, then converted to REE hydroxides with 20% NaOH (Kijkowska et al., 1989).

Zielinski et al. proposed a method for recovering REEs from the sludge of $CaSO_4 \cdot \frac{1}{2}H_2O$ (hemihydrate) generated in the production of phosphoric acid. The hemihydrate crystal was dissolved with dilute sulfuric acid and then followed by the crystallization of gypsum. The REEs passed from the crystals to the aqueous solution during the hydration reaction, allowing for them to be removed through solvent extraction. Then, the sulfuric acid with the addition of sodium sulfate was employed for the stripping and precipitation of REEs from solvent. Through the process, 80% to 85% of the lanthanides were recovered in the form of Na-REE sulfate (Zielinski et al., 1993).

El-Didamony et al. also reported the similar results in the studies of removing REEs from phosphogypsum by solvent extraction. The parameters such as the type and concentration of solvent, phase ratio and contact time were investigated. 69.8% of REEs was removed from phosphogypsum by solvent extraction (El-Didamony et al., 2011).

In addition to phosphogypsum, REEs are also enriched in phosphoric acid sludge which is generated during the evaporation process of phosphoric acid (Allaedini & Zhang, 2019). Preston et al. developed a pilot-scale process for the recovery of rare earth oxides from phosphoric acid sludge obtained in the manufacture of phosphoric acid in South Africa. The process started with acid leaching of sludge with nitric acid, where REEs reported to the leachate. Then, REEs were recovered by solvent extraction and oxalate precipitation. A mixed REE oxide of 89-94% purity was obtained through this process (J. Preston et al., 1996). Further studies also reported the processes to generate a heavy rare earth oxide with 99.4-99.8% purity, a cerium oxide with 99.98% purity and a magnet-grade neodymium oxide with 95% purity (J. Preston, 1996; J. Preston et al., 1996; J. Preston et al., 1996).

Besides sulfuric acid, apatite can also be dissolved using hydrochloric acid with $Ca(Cl)_2$ as the byproduct (Pereira & Bilal, 2012). The advantage of this approach is that $CaCl_2$ will not precipitate so that all the REEs will remain in the leachate, allowing for them to be processed directly by solvent extraction. However, the large amount of Ca makes it more difficult to obtain a high grade REE product from the leachate.

Red mud, as the main byproduct of alumina production, is rich in REEs especially Scandium. The lack of rich scandium deposits worldwide triggers numerous studies on the extraction of Scandium from red mud. Ochsenkühn-Petropoulou reported a pilot-plant process for recovery of scandium in red mud. The process starts with acid leaching of red mud to generate pregnant leachate solution, then follows the ion-exchange separation of REEs from the co-leached gangue metals such as Fe, Al, Ca, Mg, etc. After that, continues solvent extraction is employed to separate Scandium from other REEs (Ochsenkühn-Petropoulou et al., 2002).

Red mud has a high metal content, especially iron. In fact, its red color is caused by the Fe_2O_3, which is similar to the AMDp. Binnemans et al. imported dissolved SO_2 during the leaching of red mud. In the presence of SO_2, the most of Fe was kept from dissolving together with REEs. Only Na, Al and Si were leached into the solution, however, they were then separated with REEs by solvent extraction. In addition, different acids, such as HCl, HNO_3 and H_2SO_4, were compared and the best leaching efficiency was obtained with 0.5 M HNO_3. 80% of Scandium and 95% of Yttrium were recovered through the process (Binnemans et al., 2015).

Rabatho et al. have also developed a hydrometallurgical process for recovering Nd from a magnetic waste sludge generated from the Nd-Fe-B manufacturing process. The first step in the process was the preparation of PLS. The sludge was leached in HNO_3 + H_2O_2 solution at 80 ^oC to dissolve 98% Nd and while keeping the dissolution of Fe under 15%. The dissolved Fe was then removed as $Fe(OH)_3$ from PLS at pH 3. After filtration, oxalic acid was added in the filtrate for the precipitation of Nd. The precipitate was calcined at 800 ^oC to obtain Nd_2O_3 as the final product with the grade of 68%. The total recovery of Nd was 69.7% in the process (Rabatho et al., 2013).

2.2.3 The process of REE recovery from AMD

Vass conducted a comprehensive sampling program to characterize the AMD-based REE resource in 141 AMD treatment sites from Northern and Central Appalachian coal basins. The results showed that the concentration of REEs in AMDp varied from <5 to 2458 g/t with an average of 724 g/t. Fig 2.3 shows the average distribution of major elements within all these samples. It can be seen that the predominant major elements are

Si, Fe, Al, Ca, Mg and Mn, which will form the major contaminants in the following separation process (Vass, 2019).

Three unique AMDp feed stock were carefully selected from Omega, DLM, and Royal Scot AMD treatment sites for leaching procedure. The leaching tests were conducted with nitric acid and three leachates were obtained after filtration. Table 2.3 shows the elemental composition of the obtained leachates (Vass, 2019).The obtained leachate contains a large amount of co-extracted major metal ions and only a small amount of REE.

Similar to AMDp, the AMD pre-concentrate is also the precipitation product of AMD. Therefore, the study in this thesis will face the same challenge which is the recovery of REEs from the leachate with extreme low REE concentration and high content of impurities. Solvent extraction is currently viewed as the most appropriate technique for the purification and separation of rare earth due to its high extraction capacity and up-scalability (Onghena, 2018). Solvent extraction is the key of the process and its performance determines the feasibility of generating high purity REE product from AMD resource. Therefore, this thesis will focus on the development and optimization of solvent extraction process for REE recovery from AMD.

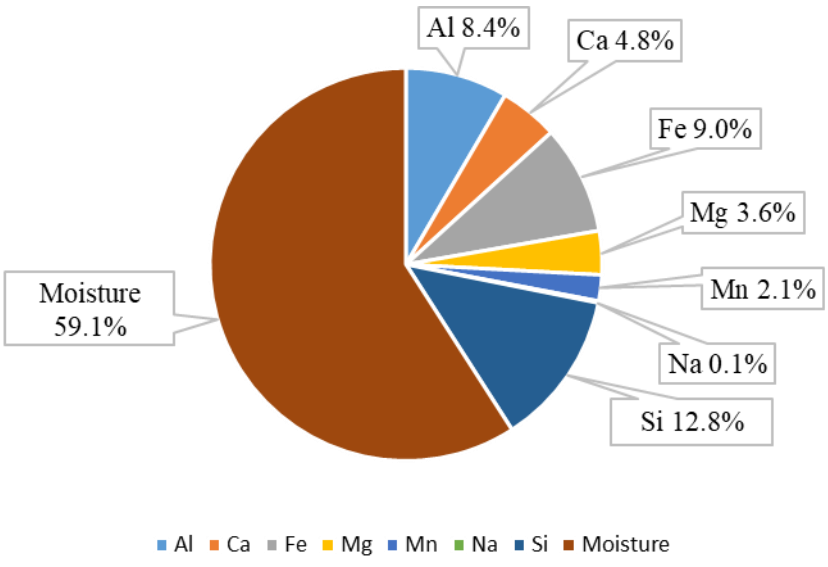

Fig 2.3 The average distribution of major elements in 141 AMDp samples (after Vass, 2019)

Table 2.3 The solution obtained from acid leaching of three AMDp samples (Vass, 2019)

Feedstock	DLM	Omega	Royal Scot
PLS pH	3.05	2.94	3.01
mg/L			
Al	9480.8	3133.4	2982.9
Ca	1401.6	1372.6	761.0
Co	103.0	18.6	22.4
Fe	1936.0	71.4	3.2
Mg	6845.6	455.2	2426.7
Mn	3,595.23	105.58	777.82
Na	47.6	12,699.5	11,493.4
Si	1274.3	59.3	53.6
SO4	497.8	25.4	881.4
Cl	17.9	5.7	4.7
TMM	25119.8	17946.7	19407.1
TREE	274.5	27.1	41.5

2.3 Solvent Extraction of REEs

2.3.1 Basics of solvent extraction

Solvent extraction (SX) is a separation method based on the preferential distribution of metals between two immiscible liquid phases when they are in contact with each other. Normally one phase is the organic, while the other one is aqueous. The distribution of the metal ions in the two phases depends on its affinity to each phase which form the basis of the selectivity in the extraction. The distribution of the metal ion is measured by *distribution coefficient D*, which is defined as the ratio of metal ion concentration in organic phase and that in aqueous phase at equilibrium:

$$D = \frac{C_{org}}{C_{aq}} \qquad 2.5$$

where C_{org} and C_{aq} denote the metal concentrations in organic phase and aqueous phase, respectively.

Instead of *distribution coefficient D*, another term *extraction efficiency E%* is commonly used to evaluate the extraction process. *E%* is defined as the percentage of a given metal ion that reports to organic phase:

$$E\% = \frac{C_{org}V_{org}}{C_{org}V_{org} + C_{aq}V_{aq}} \times 100 \qquad 2.6$$

where V_{org} and V_{aq} denote the volume of organic phase and aqueous phase, respectively.

The *extraction efficiency E%* can also be expressed by the *distribution coefficient D*:

$$E\% = \frac{D}{V_{aq}/V_{org} + D} \times 100 \qquad 2.7$$

If there are two metal ions A and B, the D_A and D_B are different, which give the information to the separation of metal A and B in a certain extraction system. The separation of the extraction is quantified by the *separation factor α*, which is given by:

$$\alpha_{A/B} = \frac{D_A}{D_B} \qquad 2.8$$

It is very difficult to separate metal ions if *separation factor α* is close to 1, and good separation is achievable if *separation factor α* is either much larger than 1 or less than 1.

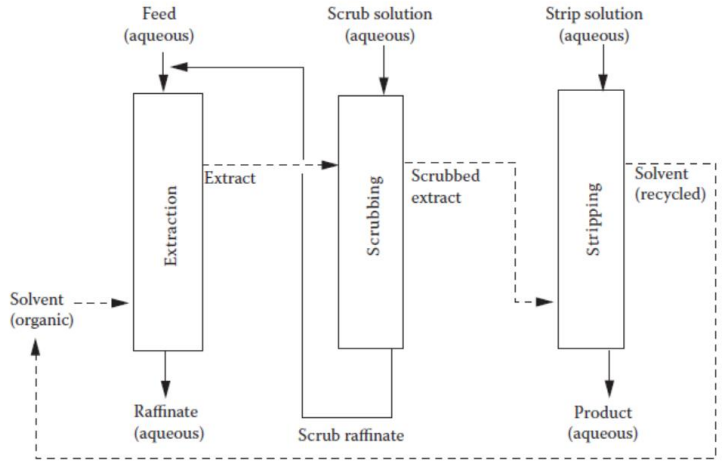

Fig 2.4 schematic of solvent extraction process (after Gupta and Krishnamurthy, 1992)

The schematic of solvent extraction process is shown in Fig 2.4. The extraction stage is performed by transferring the metal ions in aqueous phase to the organic phase. The organic phase usually consists of an extractant, a diluent and optionally a modifier (Free, 2013). The extractant is the active component to extract metal ions into the organic phase (Jack Zhang et al., 2016). Metal ions prefer to stay in the aqueous phase due to the hydration reaction. The extractant is able to coordinate to the metal ion and form a metal-extractant complex with preference of dissolving in the organic phase. The extractant shows selectivity in the extraction which allows the separation of different metal ions.

The extractant is generally viscous so that it is necessary to dissolve it in a diluent to ensure the good contact between the organic phase and aqueous phase (Krishnamurthy & Gupta, 2004). The diluent may also affect the extraction equilibrium since the interaction between the diluent and metal-extractant complex. In some conditions, a substance known as a modifier is also added in the organic phase to improve the phase disengagement.

After extraction, the loaded organic solution is washed by the water, dilute acid or base solution to remove the undesirable impurities co-extracted with target metal ions, which is called scrubbing stage. The extraction conditions are controlled precisely to remove the impurities while the targeted metal ions remain in the organic phase. If the scrubbing solution contains a high amount of targeted metals, the scrubbing solution will be recycled, i.e., going back to the extraction stage (Jack Zhang et al., 2016).

Stripping is the reverse operation of extraction. In this stage, the rare earth metal is back-extracted to a stripping solution from the loaded organic phase. Stripping is normally undertaken with concentrated salt, acid, or alkaline (Krishnamurthy & Gupta, 2004). The stripping conditions are determined by the type of extraction system.

2.3.2 Type of extraction system

The extraction system of rare earth can be classified as cation extraction, anion extraction and solvating extraction based on the type of the extractants (Jack Zhang et al., 2016). The metal is extracted as a metal cation M^{n+} in acidic extraction, as a metal anion MX_x^{n-} in anion extraction and a neutral metal salt MX_n in solvating extraction (Wilson et

al., 2014). Solvent extraction of rare earths has been reviewed by Xie et al. and the commercial extractants are summarized in Table 2.4.

Table 2.4 Extractants for solvent extraction of rare earth

(Xie, Zhang, Dreisinger, & Doyle, 2014)

Extractant Type	Reagent Class	Structure	Industrial Names
Cation extractants	Carboxylic acids	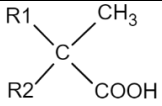	Versatic 10, versatic 911
	Phosphorous acids	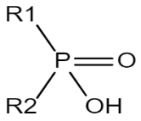	D2EHPA, EHEHPA, HEHEHP, P507, PC88A, P229, Cyanex 272
Solvating extractants	Phosphorous ester and oxides	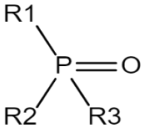	TBP, DBBP, TOPO, Cyanex 921
Anion extractants	Primary amines	RNH_2	Primene JMT, N1923
	Quaternary amines	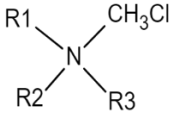	Aliquat 226, Adogen 464

(1) Acidic extraction

Acidic solvent extraction uses the organic acid to extract metals through cation exchange. The overall reaction can be expressed as below (Peppard, Mason, Driscoll, & Sironen, 1958).

$$M^{3+} + 3\overline{HA} = \overline{MA_3} + 3H^+ \qquad 2.9$$

where *M* denotes rare earth ion and *A* denotes the organic anion. The distribution ratio *D* can be expressed as:

$$\log D = \log K + 3\log[HA] + 3pH \qquad 2.10$$

According to the equation above, in acidic solvent extraction system, distribution ratio is subjected to the effects of equilibrium constant (K), extractant concentration (HA) and pH. The equilibrium constant (K) is related to the factors like the properties of extractant and diluent, the metal ion species *etc*. (Jack Zhang et al., 2016).

Acidic organic phosphorous extractants have been studied in the solvent extraction of REEs. Di-2-ethyl-hexyl-phosphoric acid (D2EHPA) and 2-thyl-hexyl-phosphonic acid mono-2-ethylhexyl easter (EHEHPA, HEHEHP, P507, PC88A) are widely used. Battsengel et al. have studied the recovery of REEs from an apatite ore sample by solvent extraction with D2EHPA. 85% of light REEs and 89% of heavy REEs were dissolved in the solution with 1 M H2SO4 in an hour. The heavy REEs present in the pregnant leach solution were almost entirely extracted using 1.2 M D2EHPA as a cation exchanger, while most of the light REEs remained in the raffinate. The heavy REEs loaded into the organic phase were stripped completely by 3 M H_2SO_4 solution. The light REEs in the raffinate precipitated as REE oxalates by the addition of 0.08 M oxalic acid (Battsengel et al., 2018). The EHEHPA or HEHEHP, known as P507 and PC88A in market, was also extensively investigated. The advantage of these extractants is that the stripping of REEs can be conducted at lower acidity than that in D2EHPA (Reddy, Prasada Rao, & Damodaran, 1993).

Carboxylic acids are widely used for separating yttrium from lanthanides because the extraction of yttrium is different for these reagents. For example, yttrium is extracted with light rare earths with napthenic acids while it is extracted with middle rare earths with Versatic 10 (J. S. Preston & Du Preez, 1998).

(2) Anion extraction

In anion extraction system, a negatively charged complex is formed by the reaction of metal ions with inorganic ligands, which is then extracted to organic phase by organic cations. Amine compounds are commonly used in this type of system. The extraction process is usually described as liquid anion exchange. Primene JMT (tri-alkyl methylamine) is a typical anion exchanger used in rare earth extraction. When it is used in the extraction of lanthanum from sulfate solutions, the reaction can be expressed as (El-Yamani & Shabana, 1985):

$$2\overline{RNH_2} + \overline{H_2SO_4} = \overline{(RNH_3)SO_4} \qquad 2.11$$

$$2M(SO_4)_3^{3-} + 3\overline{(RNH_3)_2SO_4} = 2\overline{(RNH_3)_2M(SO_4)_3} + 3SO_4^{2-} \qquad 2.12$$

where RNH_2 denotes the Primene JMT in the organic phase.

According to the reaction equation, it can be seen that the key point of the extraction lies in the formation of anionic complex $M(SO_4)_3^{3-}$ but not the affinity of metal ion for the extractant itself.

Another typical anion exchanger is Aliquat 336. When it is use to extract REEs, the extraction efficiency of LREEs are higher than that of HREEs. This behavior is different from that of the cation and solvating extractants, for which the extraction efficiency of HREEs is higher than that of LREEs (Xie et al., 2014). Hence, this extractant can provide a method to separate LREEs from solutions.

(3) Solvation extraction

The solvating extraction is a neutral process. The extractant firstly replaces the water molecules surrounding metal ions with organic solvent molecules to facilitate organic solubility. Then, a neutral complex is formed through a coordinate bond between the metal and the polar oxygen atoms of extractant. The extraction of rare earths in nitrate system by using tri-butyl phosphate can be expressed by the equation below.

$$M^{3+} + 3NO_3^- + 3\overline{TBP} = \overline{M(NO)_3(TBP)_3} \qquad 2.13$$

The distribution ratio *D* can be expressed as:

$$D = K(NO_3^-)^3(TBP)^3 \qquad 2.14$$

Equation 2.14 shows that the distribution ratio increases with the increasing of extractant and salt concentrations. The solvation extractants that have been used for rare earth separation are tri-butyl phosphate (TBP) and di-butyl-butyl-phosphonate (DBBP). Preston et al. described a pilot-scale process to recover REEs from the byproduct in phosphoric acid production. 85% of REEs were recovered by acid leaching with nitric acid and the REEs were then extracted into 33 vol% DBBP. The organic phase was then stripped with water to yield a solution of REE nitrates. The mixed REE oxide with 98% purity was obtained by oxalate precipitation and calcination (J. Preston et al., 1996). Further studies were conducted on the development of a solvent extraction process to separate cerium (IV) from the mixed REEs oxides (J. Preston et al., 1996). The first step was the dissolution of the mixed oxide in the concentrated nitric acid. After dilution with water, the cerium (IV) was selectively extracted in to 15 vol% TBP while the trivalent

REEs was remained in the leachate. Finally, a cerium dioxide of 99.98% purity was obtained through the process. Peppard et al. also compared the REE extraction with TBP from nitrate and chloride solutions. The results showed a better extraction ability of TBP in the nitrate solutions (Peppard et al., 1958).

2.4 Summary

Rare earth elements (REEs) are essential for the modern technologies from cell phones, electric cars, satellites to defense aircraft. U.S. consumed around 11% of global demand of REEs and 80% of the REEs imported from China in 2015. Without domestic supply chain, the U.S. is vulnerable to the changes in the international market. Therefore, the U.S. Department of Energy (DOE) conducts several programs to study on the REE recovery from coal and byproducts.

Our research team focus on the extraction of REEs from the AMD, which is discharged during or after coal production. AMD have been described as the largest environment problem for the coal areas. Researchers in WVU evaluated the REE reserves at hundreds of AMD treatment sites in Appalachian coal basin. It is estimated that more than 45000 tons of REEs can be generated per year only in the area of Pennsylvania and West Virginia, which is three times the current domestic demand for REEs. Therefore, our efforts are made not only to strengthen resource independence, but also to promote the fuel economic and reduce the environmental pollution.

The existing literature has shown a lot of work on REEs recovery from the rare-earth-containing industrial residues, such as the phosphogypsm, phosphoric acid sludge and red mud. However, limited efforts are made on acid mine drainage. A lot of hydrometallurgical methods have been developed for REEs recovery while these techniques including leaching and solvent extraction are only commercially applied to the production of conventional REEs deposits. Additional study is required to adapting these techniques to the new feedstock AMD. Solvent extraction is currently viewed as the most applicable method for the purification and separation of rare earth. Hence, a detailed study will be conducted on the development of solvent extraction process to recover REEs from AMD.

Chapter 3. Evaluation of Solvent Extraction Operating Parameters using Synthetic REE Solutions

3.1. Introduction

The objective of this study was to investigate the recovery and transport of REEs in solvent extraction through controlled laboratory batch tests using artifical solutions. Rather than individually assess all 17 REEs, the experimental program was simplified to only assess five surrogate REEs, namely Yttrium (Y), Cerium (Ce), Neodymium (Nd), Dysprosium (Dy) and Scandium (Sc). These surrogate elements were carefully selected to include a mix of light REEs (Ce and Nd), heavy REEs (Y and Dy), those that tend to be anomalously concentrated in aqueous sources (Y and Ce), and those that command the highest market value (Sc). In this study, the artificial leachate solution was accessed to study how a variety of parameters affected the extraction and stripping of these surrogate REEs. The optimal solvent extraction conditions for the five REEs was determined.

3.2. Methodology

3.2.1 Materials

(1) Aqueous solutions

Synthetic leachate solutions of Y(III), Nd(III), Dy(III), Sc(III), Ce(IV) were prepared by diluting the standard solutions from Inorganic Ventures, Inc. The target concentration of each artificial leachate was 40 mg/L, and these values were confirmed by ICP-MS (Thermo Electron, iCAP RQ). The results from these analyses are shown in Table 3.1.

Table 3.1 Concentrations of REE in the feed solutions.

Elements	Sc(III)	Y(III)	Ce(IV)	Nd(III)	Dy(III)
Concentration, mg/L	36.18	36.78	39.04	39.09	36.95

(2) Selection of extractant

Researchers have investigated a lot of extractants on the solvent extraction of REEs. However, only a small amount of them are used commercially. Di-2-ethyl-hexyl-phosphoric acid (D2EHPA), 2-ethyl-hexyl-2-ethyl-hexyl-phosphonic acid (EHEHPA), Versatic acid (Versatic 10), tri-butyl phosphate, and Aliquat 336 have been widely used in rare earth industry due to their good extraction ability and low operational cost (Ismail, Aziz, Yunus, & Hisyam; Xie et al., 2014).

As discussed above, the leachate generated by acid leaching of AMDp is at low pH and contains significant amount of metal impurities such as Fe, Al, Ca, Mg, and Mn. The presence of the impurities will increase the cost and difficulty of solvent extraction process. Therefore, the most appropriate extractant should be able to be effective at low pH and with the features of low price, high extraction efficiency of REEs, and the effective separation of REEs from impurities.

Aliquat 336 is an anion extractant. The key point of the extraction lies in the coordination of metal ions with inorganic ligands (SO^{4-}, Cl^{-}, NO^{3-}) in the aqueous phase but not the affinity of metal ion for the extractant itself. The abound of metal ions like Fe^{3+}, Al^{3+}, Mg^{2+}, Mn^{2+} will compete with REE ions to coordinate with the inorganic ligands. Besides, Aliquat 336 is a relatively weak extractant for REEs compared to some cation extractants (EHEHPA and HDEHP) and high concentration of salts and acids are required to achieve a good separation (Krishnamurthy & Gupta, 2004). As a result, Aliquat 336 is not suitable for the solvent extraction of REEs from AMDp.

The same problem also lies in the extraction with tri-butyl phosphate, which is a kind of solvation extractants of which the inorganic ligands also participate in the extraction process. The demand for a large amount of salts in extraction will increase the operation cost on scale-up process.

D2EHPA and EHEHPA are organophosphorus acids and Versatic 10 is versatic acid, which are categorized as cation extractants. One advantage of cation extraction is that the extraction and stripping of metal ions can be controlled by pH. However, Versatic 10 has a very broad pH swing between 0% extraction and 100% extraction which make it difficult to separation different metal ions. Versatic 10 is able to form very

stable complexes with Fe^{3+} (Wilson et al., 2014). In other words, Versatic 10 is not good at separating REEs with a large amount of multiple metal ions including Fe^{3+}. Among organophosphorus acids, D2EHPA has proven to be the most versatile extractant with chemical stability, good performance of extraction, loading and stripping as well as low solubility in aqueous phase. Compared to EHEHPA, D2EHPA shows a better extraction of TREEs from leach liquor bearing metals of Mn, Cu, Fe, Co and Ni (Parhi, Park, Nam, & Park, 2015).

Therefore, D2EHPA was used as the main extractant in the study on REE recovery from AMDp by solvent extraction.

The extractant was dissolved in kerosene to obtain different concentrations. Kerosene is a non-polar diluent and has been proven to be a good choice for the solvent extraction of REEs, because it can give highest equilibrium constant when compared to other diluents like n-hexane, benzene, and chloroform (Zhang et al., 2016).

In addition to kerosene, a group of commercial diluents, Elixore range solvent (supplied by Total Special Fluids, Inc., Houston, TX) were tested to seek better choice of diluent.

Tri-n-butyl phosphine was used as the modifier. Tri-butyl phosphine is easily oxidized by air to tri-butyl phosphine oxide (TBPO) (Armarego, 2017). Solvent extraction experiments were conducted in the atmosphere and the aqueous phase contained nitric acid, which set up a strong oxidation environment. Therefore, it was believed that tri-butyl phosphine was oxidized to TBPO in solvent extraction.

3.2.2 Experimental procedures

Solvent extraction and stripping experiments were carried out in 125 mL separatory funnels at room temperature. The pH of the aqueous solution was adjusted to the desired value by adding sodium hydroxide (NaOH) solution or nitric acid (HNO_3). In each experiment, the aqueous feed solution and the organic phase containing extractant were added into a separatory funnel, which was agitated by a mechanical shaker (Yamato, SA320 shown in Fig 3.1) with different shaking times. After achieving

equilibrium, the aqueous phase was separated from the organic phase by discharging the former from the separatory funnel.

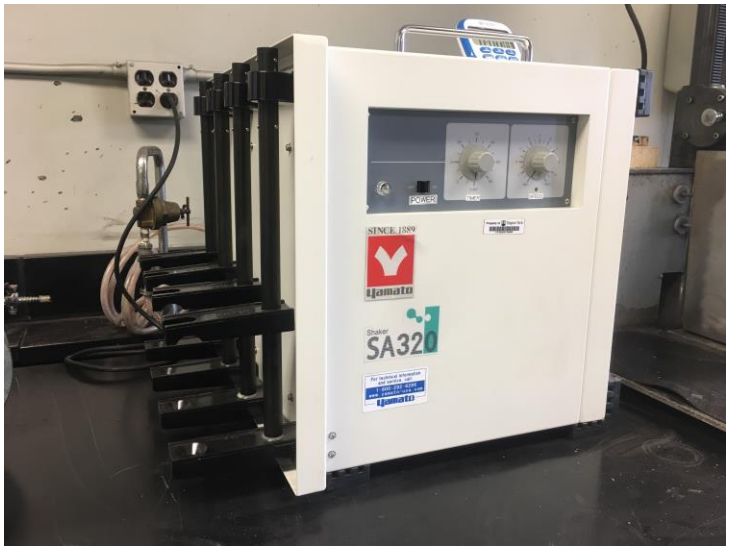

Fig 3.1 Yamato SA320 horizontal-vertical laboratory shaker

The REE concentration in the aqueous phase was measured directly by ICP-MS, while the REE in organic phase was determined by the mass balance. The extraction efficiency *%Extraction* and stripping efficiency *%Stripping* were calculated to evaluate the extraction and stripping, respectively, which is given by Equation 3.1 and 3.2:

$$\%Extraction = \frac{C_O V_O}{C_O V_O + C_A V_A} \times 100 \qquad 3.1$$

$$\%Stripping = \frac{C_A V_A}{C_O V_O + C_A V_A} \times 100 \qquad 3.2$$

where C_A and C_O represent the concentration of metal ions in the aqueous and organic phase, respectively. V_A and V_O are the volumes of the aqueous phase and organic phase, respectively.

3.2.3 Extraction Mechanism

The mechanism by which D2EHPA extracts REEs from the aqueous phase is detailed here. It is well known that D2EHPA exists as dimmers in nonpolar organic

diluents. Generally, the extraction of REE in trivalent state from aqueous phase by D2EHPA can be expressed by the cation exchange reaction as below:

$$RE^{3+} + 3(HX)_2 \rightleftharpoons \overline{REX_3(HX)_3} + 3H^+ \quad 3.3$$

The extraction equilibrium constant K is expressed by:

$$K = \frac{[\overline{REX_3(HX)_3}][H^+]^3}{[RE^{3+}][(HX)_2]^3} \quad 3.4$$

As the distribution coefficient *D* is expressed by,

$$D = \frac{[\overline{REX_3(HX)_3}]}{[RE^{3+}]} \quad 3.5$$

The *D* can also be expressed by the *equilibrium constant K and pH,*

$$\log D = \log K + 3\log[HX] + 3pH \quad 3.6$$

According to the equation above, in acidic solvent extraction system, distribution ratio is subjected to the effects of equilibrium constant (K), extractant concentration (HX) and pH. The equilibrium constant (K) is related to the factors like the properties of extractant and diluent, the metal ion species *etc*. (Jack Zhang et al., 2016).

3.3 Results and Discussion

3.3.1 Effect of reaction time

To investigate the influence of reaction time, a series of solvent extraction experiments were conducted using artificial solution only containing Y(III) at varied reaction times, namely 5 min, 10 min and 15 min. Fig 3.2 shows the effect of reaction time on extraction efficiency of Y(III). As shown in Fig 3.2, the extraction efficiency does not change from 10 min to 15 min, indicating that the equilibrium of solvent extraction can be reached within 10 min. This value was thus used in all subsequent tests.

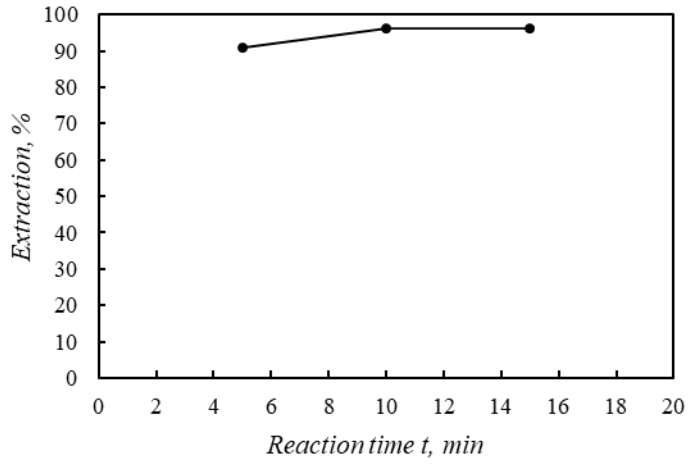

Fig 3.2 Effect of reaction time on the extraction efficiency of Y(III)

c(D2EHPA) = 0.025 M; pH = 0.5; V_A:V_O=1:1.

3.3.2 Effect of the concentration of REEs in the Feed

Preliminary tests had shown that the extraction efficiency of Dy (III) was more sensitive to the experimental parameters, i.e., the concentration of extractant, than other REEs. Therefore, Dy (III) was selected to investigate the effect of feed concentration on solvent extraction. The experiments were carried out by varying Dy(III) concentration from 1 to 1000 mg/L with 0.2 M D2EHPA at an initial pH of 2. As described by Huang et al. and Chiou et al., the driving force for the mass transfer becomes stronger with the increase of the feed concentration, and as a result, higher extraction efficiencies are expected for higher feed concentrations (Chiou & Li, 2002; Huang, Bin, Bu, Jiang, & Zeng, 2011). Fig 3.3 shows that the extraction efficiency increases with the increase of feed concentration from 1 to 200 mg/L and the extraction efficiency is essentially 100% for all concentrations greater than 200 mg/L. Therefore, the concentration of total REEs in the artificial solution used in the following parametric study is set at 200 mg/L.

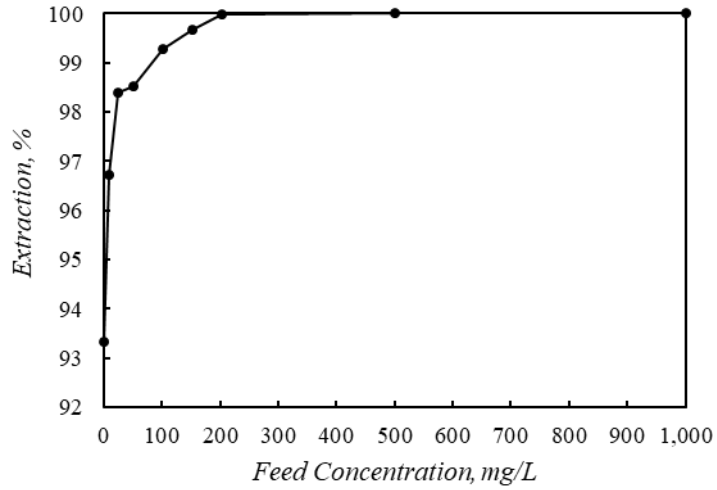

Fig 3.3 Effect of feed concentration on the extraction efficiency of Dy(III).

pH = 2; c(D2EHPA) = 0.2 M; V_A/V_O*=1:1; t = 10 min.*

3.3.3 Effect of D2EHPA concentration, c(D2EHPA)

A test series was conducted to study the effect of D2EHPA concentration on the extraction of REEs. The selected concentrations of D2EHPA were 0.025, 0.05, 0.1, 0.2 and 0.3 M. The results showed that the extraction efficiency of Sc(III), Y(III), Dy(III), Nd(III) and Ce(IV) increased with increasing the concentration of D2EHPA (Fig 2.4). According to Equation 3.6, the *D* is proportional to the third power of the extractant concentration. Thus, a higher concentration of extractant facilitated the extraction of REEs.

The extraction of the five REEs with D2EHPA from nitrate media follows the order of $\mathrm{Ce(IV) < Nd(III) < Dy(III) < Y(III) < Sc(III)}$, which is due to that REEs with less basicity will form more stable complexes. Therefore, REEs with less basicity can be extracted more easily. Krishnamurthy and Chiranjib reported the basicity order of all REEs, i.e., (Krishnamurthy & Gupta, 2004)

$$\mathrm{La^{3+} > Ce^{3+} > Pr^{3+} > Nd^{3+} > Pm^{3+} > Sm^{3+} > Eu^{3+} > Gd^{3+} > Tb^{3+} > Dy^{3+} > Ho^{3+} > Y^{3+}\ Er^{3+} > Tm^{3+} > Yb^{3+} > Lu^{3+} > Sc^{3+}}$$

At pH = 0.5, the extraction efficiency of Nd(III) and Ce(IV) was very low, suggesting that Nd(III) and Ce(IV) were too difficult to extract with D2EHPA at this pH, which

provided the possibility that separate Nd(III) and Ce(IV) from Y(III), Sc(III) and Dy(III) by controlling pH (Fig 3.4).

For all the five REEs, no obvious increase in the extraction efficiency was observed in the range of 0.2-0.3 M (Fig 3.4). Therefore, the optimum concentration of D2EHPA was set at 0.2 M.

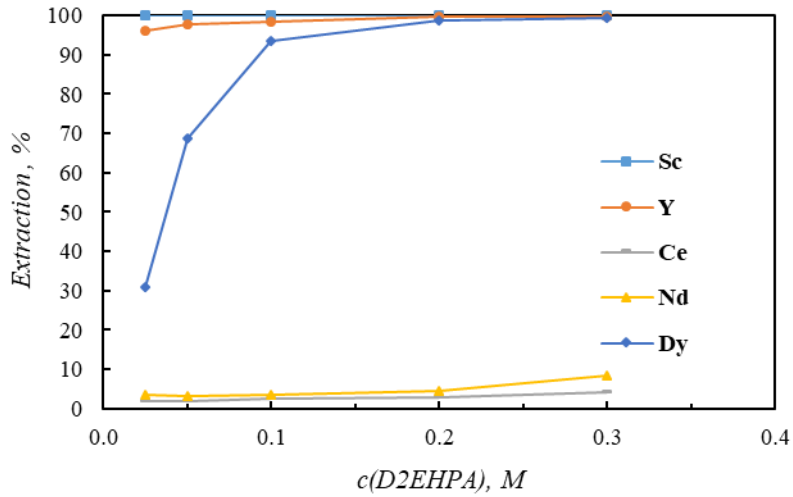

Fig 3.4 Effect of D2EHPA concentration on the extraction efficiency of REEs.

pH = 0.5; V_A/V_O=1:1; t = 10 min;

3.3.4 Effect of initial pH in aqueous phase

The second test series evaluated the influence of initial pH in aqueous phase. Solvent extraction experiments were carried out at different pH values, namely 0.5, 1.0, 1.5, 2.0, 3.0, 4.0 (Fig 3.5). According to Equation 3.6, the distribution coefficient was proportional to the third power of the pH value, which indicated that a higher pH facilitated the extraction of REEs. All the Y(III) and Dy(III) were completely extracted when pH was larger than and equal to 1. Nd(III) and Ce(IV) were completely extracted when pH was equal to or larger than 2. Therefore, the optimum pH for full extraction was determined to be 2.0.

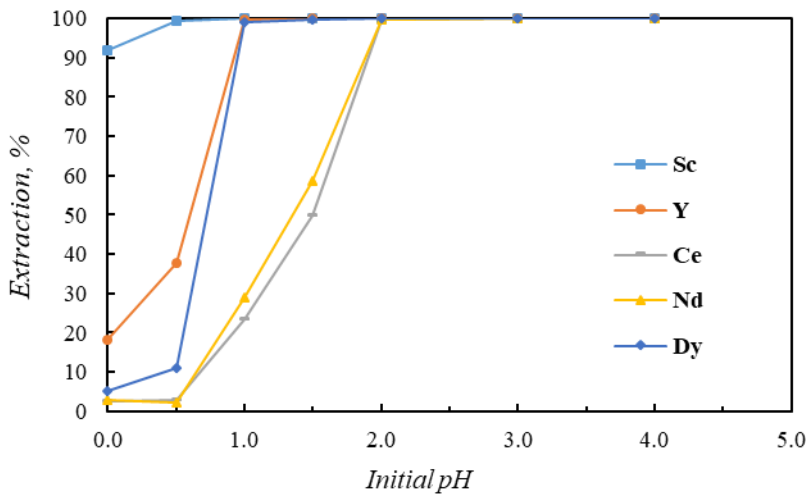

Fig 3.5 Effect of initial on the extraction efficiency of REEs.

C(D2EHPA) = 0.2 M; V_A/V_O=1:1; t = 10 min.

3.3.5 Selection of diluent

While much of the prior testing has used kerosene as a generic diluent, further testing was conducted to evaluate several specialty diluents. Like most organic solvents, kerosene is highly volatile and flammable. The moderate aromatic content also produces a foul odor and potential health effects. Altogether, an optimal diluent should not only produce superior technical performance but should also balance any significant health, safety, and environmental concerns.

Table 3.2 Technical Data for Elixore Diluents (after Elixore, 2014) and Kerosene (Wikipedia)

Parameter	Unit	Elixore 205	Elixore 230	Elixore 250	Kerosene
Flash Point PM	° C	76	103	119	37-65
Aromatic Content	ppm	40	40	40	<25
Sulfur Content	ppm	<1	<1	<1	<4
Vapor Pressure at 20° C	kPa	0.016	0.002	0.0003	0.7

As an alternative to kerosene, the Elixore range is a group of aliphatic diluents designed specifically for the liquid-to-liquid extraction process (Elixore, 2014). Compared to the kerosene, the diluents in the Elixore range have higher flash points and lower evaporation rates. They offer a good balance between phase separation, diluent losses, and fire risk. In addition, the low aromatic content and high flash points also help

enhance worker safety and meet strict environmental requirements compared to kerosene-type diluents with a mixture of aromatic and aromatic.

In the present work, three diluents namely, Elixore 205, Elixore 230 and Elixore 250, were investigated to replace kerosene as the diluent in the extraction of REEs. As shown in Fig 3.6, the new diluents performed comparably than kerosene in the extraction of Y(III), Dy(III), Nd(III), Sc(III) and Ce(IV). Given these factors and availability, Elixore 205 was selected as the primary diluent for future tests.

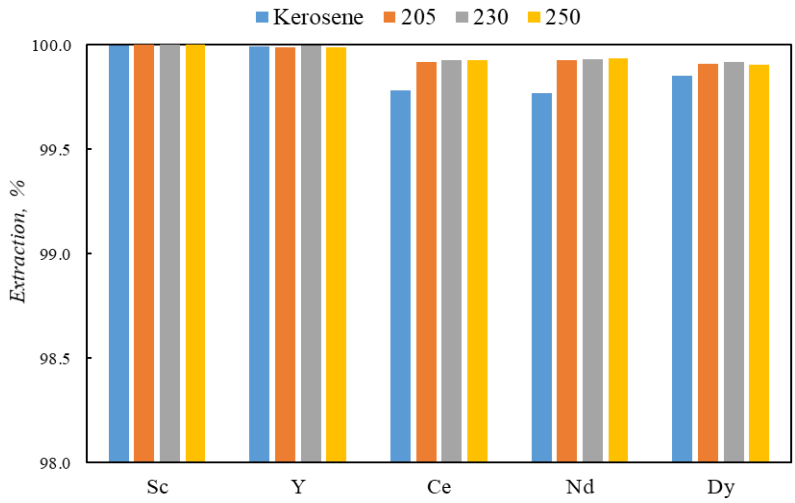

Fig 3.6 Comparison between Kerosene and Elixore Range of the extraction efficiency of REEs.

c(D2EHPA) = 0.2 M; pH = 2; V_A/V_o =1; t = 10 min.

3.3.6 Selection of stripping reagent

Solvent stripping tests were conducted using different concentrations of HNO_3 (0.1-7 M) and HCl (0.1-7 M) at a 1:1 phase ratio. The loaded organic phase used as feed in these tests was obtained from the extraction experiments using 0.2 M D2EHPA in Elixore 205 at an initial pH 2 and a phase ratio of 1:1.

Fig 3.7 show that the stripping efficiency increases with increasing acid concentration, which is consistent with general expectations and previous studies (X. Sun, Zhao, Meng, & Li, 2005). Using HCl as the stripping reagent, the stripping efficiency increases as the HCl concentration is increased from 0.1 M to 6 M, however, further increases above 6 M do not promote higher stripping efficiency. Likewise, HNO_3 follows a similar trend, reaching the maximum efficiency at 5 M. When analyzing the

results element-by-element, Ce(IV) and Nd(III) show no significant difference between the two acid types; however, both of these are also easily stripped in general. Alternatively, the stripping efficiencies of Y(III) and Dy(III) using HCl are higher than that using HNO_3 at the same concentration, indicating that HCl is more efficient than HNO_3 as a stripping reagent. Sc(III) was notably difficult to strip, even at the highest acid concentrations tested, 7 M.

In general, the higher the extractability of the REE is, the more difficult the REE can be stripped from the loaded extractant. This behavior is also confirmed by the results shown in Fig 3.7. The order of stripping of REEs, namely Ce(IV) > Nd(III) > Dy(III) > Y(III) > Sc(III), is the reverse of the order of extraction. When the acid concentration was 0.5 M, it was found that most of Sc(III), Y(III), Dy(III) could not be stripped whereas the stripping efficiencies of Nd(III) and Ce(IV) were both more than 90%. Therefore, it may be possible to separate various REEs by controlling the acidity in stripping system.

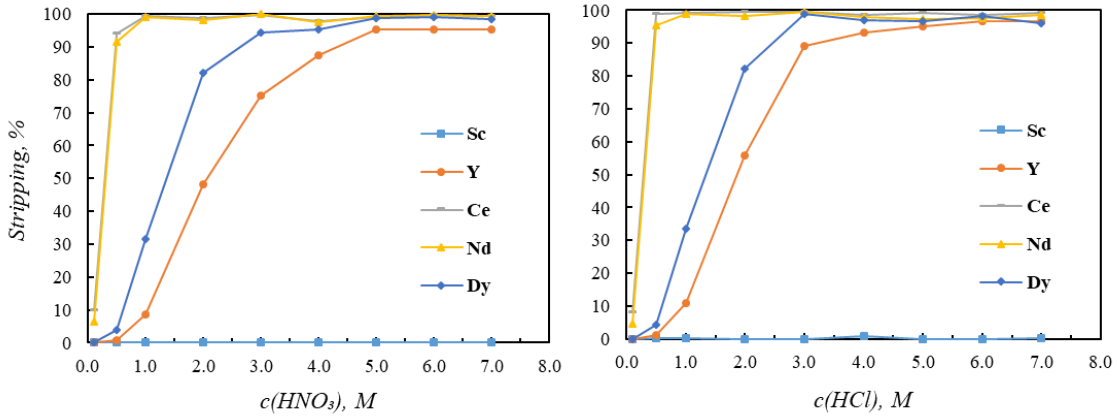

Fig 3.7 Effect of acid concentration on the stripping efficiency.

V_A/V_O=1; t = 10 min.

3.3.7 Effect of modifier on the solvent extraction system

(1) Effect on the stripping of Sc(III) with sodium hydroxide (NaOH)

Due to the strong affinity between scandium (Sc) and the D2EHPA, the stripping efficiency of Sc from D2EHPA is very low, even with strong acids (Wang, Pranolo, & Cheng, 2013). An alternative method is to directly precipitate Sc(III) from organic in the form of $Sc(OH)_3$. To evaluate this approach, the stripping tests of Sc(III) were conducted

using 2 M NaOH at phase ratio of 1:1. During these tests, an emulsion layer appeared in the stripping solution between the organic and the aqueous phases (Fig 3.8). After stripping, 61.15% of Sc(III) was recovered to the emulsion while only 23.99% of Sc(III) was in the aqueous strip solution (Table 3.3). Downstream recovery of Sc(III) from the emulsion is impractical; therefore, a phase modifier must be added to the organic solvent to help phase separation due to emulsification.

As a result, TBPO was evaluated as the modifier to help phase separation in the Sc stripping stage. The loaded organic phase used as the feed in the test was obtained from the extraction experiment using 0.2 M D2EHPA and 0.1 M TBPO in Elixore 205 at an initial pH 2 and a phase ratio of 1:1. As shown in Fig 2.11, the modifier helped the phase separation and the precipitation of $Sc(OH)_3$. The precipitate $Sc(OH)_3$ in the aqueous phase was then separated from the organic phase and dissolved in the acid for ICP-MS analysis. As shown in Table 3.3, the stripping efficiency of Sc(III) increased to 75.04% by adding TBPO. The results are promising and represent a dramatic improvement over the acid stripping.

Table 3.3 The distribution of Sc(III) in the stripping process

	Organic phase,%	Emulsion,%	Aqueous phase/Solid,%
Without Modifier	14.85	61.15	23.99
With Modifier	24.96	--	75.04

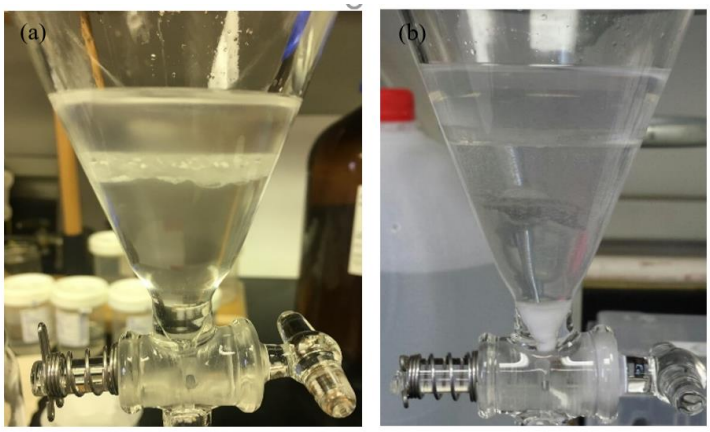

Fig 3.8 Stripping Solution (a) Without TBPO (b) With TBPO

c(D2EHPA) = 0.2 M, c(TBPO) = 0.1 M, c(NaOH) = 2 M, V_A/V_O=1; t = 10 min.

(2) Effect on the solvent extraction of REEs

In order to investigate the influence of the interaction between TBPO and D2EHPA on the extraction of REEs, experiments were conducted by using 0.2 M D2EHPA containing various TBPO concentrations, namely, 0, 2.5 and 5 vol.%. As shown in Fig 3.9, the extraction of the five REEs follows the order of Ce(IV) < Nd(III) < Dy(III) < Y(III) < Sc(III) under all the concentrations of TBPO. This result indicates that the addition of TBPO does not change the extraction order of the five REEs with D2EHPA.

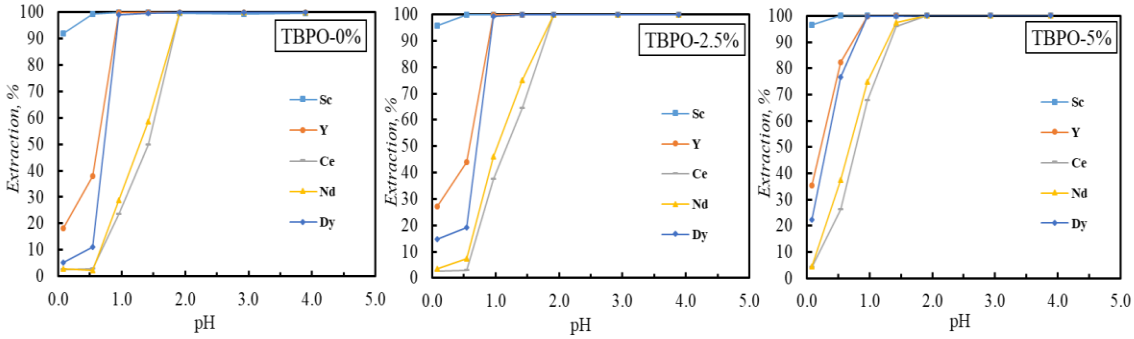

Fig 3.9 Effect of pH on the extraction efficiency of Sc(III), Ce(IV), Nd(III), Dy(III) and Y(III) at different TBPO concentrations

c(D2EHPA) = 0.2 M; $V_0/V_A=1$; T = 298 K; t = 10 min.

Fig 3.10 shows the effect of TBPO concentration on the extraction of five REEs. As shown in Fig 3.10. the presence of TBPO causes the extraction curves of Y(III), Nd(III), Dy(III) and Ce(IV) to shift towards lower pH values. In other words, the extraction efficiency of the four REEs increase with the increase of TBPO concentration at a given pH value. Although the extraction efficiency of Sc(III) is more than 90% in all cases, a slight increase can also be observed at pH 0.1 with the increase of TBPO concentration. The results confirm that the addition of TBPO improve the extraction of all five REEs.

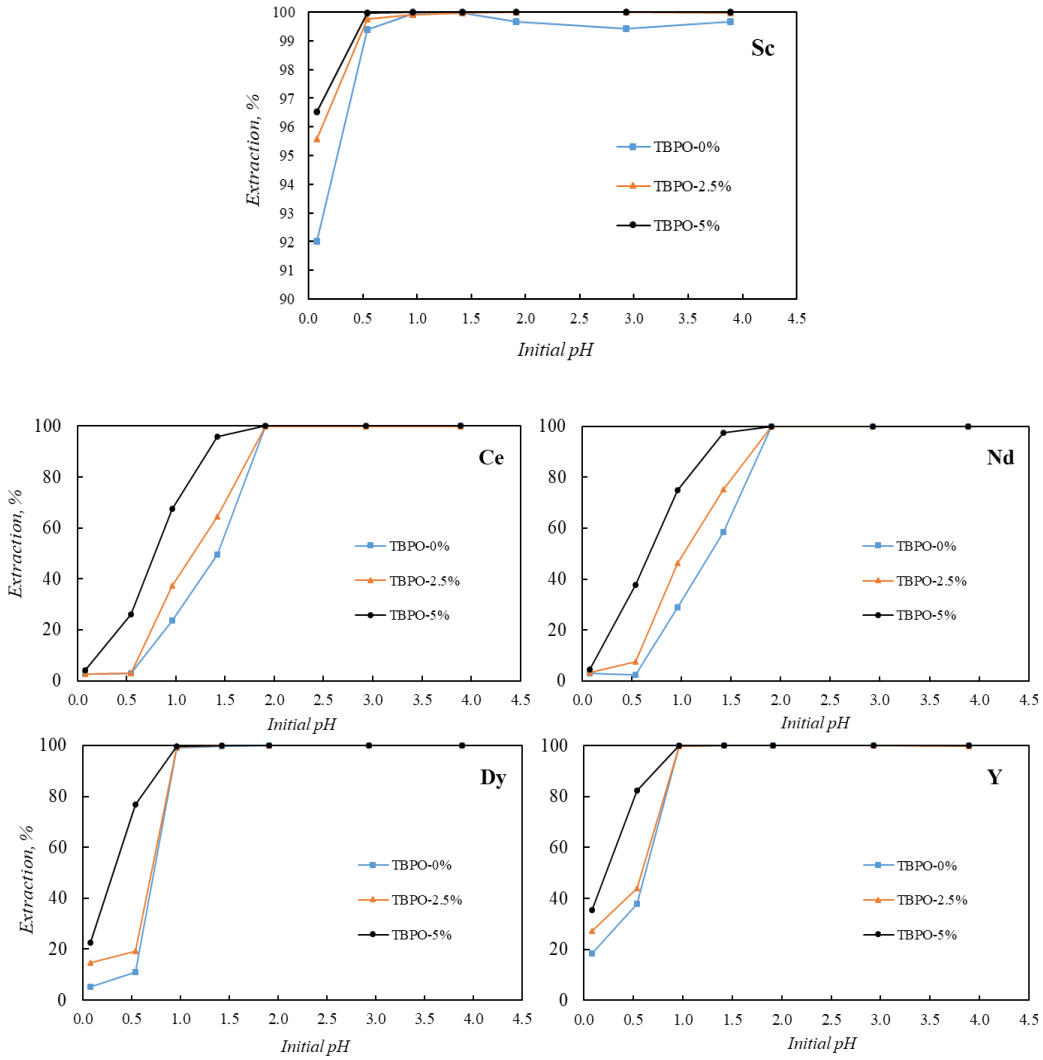

Fig 3.10 pH-extraction isotherms of Ce(IV), Nd(III), Dy(III), Y(III) and Sc(III) at different TBPO concentrations

c(D2EHPA) = 0.2 M; V_A/V_o*=1; t* = 10 min.

2.4 Conclusions

In this chapter, parametric study was conducted on the recovery of five surrogate REEs in the solvent extraction with D2EHPA. The results indicated that the extraction and stripping of REEs were determined by various parameters including reaction time, feed concentration, D2EHPA concentration, aqueous pH, type of diluent, addition of

modifier, the type and concentration of stripping reagent. Specific findings are listed below.

1) D2EHPA can be used to extract the REEs of Sc(III), Ce(IV), Nd(III), Dy(III) and Y(III) efficiently. The extraction of the five REEs with D2EHPA from nitrate media follows the order of Ce(IV) < $\mathrm{Nd(III) < Dy(III) < Y(III) < Sc(III)}$ and the extraction efficiency increases with the increase of aqueous pH and D2EHPA concentration.
2) Elixore 205 is proven a better choice of diluent than kerosene due to its high performance in the extraction of REEs as well as in the safety evaluation.
3) HCl and HNO_3 can be used to recover Ce(IV), Nd(III), Dy(III) and Y(III) from D2EHPA. Their stripping efficiency in both acids increases with the increase of acid concentration and HCl provides better recovery of REEs.
4) The use of NaOH provides a practical method to recover Sc(III) from D2EHPA by forming $Sc(OH)_3$ precipitate in the stripping stage.
5) The addition of modifier will not only help the extraction of REEs but also the phase separation in stripping of Sc(III) with NaOH.

Based on the information above, the optimal chemical conditions are determined. Nearly 100% extraction efficiency of REEs can be obtained when solvent extraction experiments are conducted with 0.2 M D2EHPA + TBPO in Elixore 205 at pH 2. After extraction, 6 M HCl is employed to recover REEs from organic and nearly 100% stripping efficiency can be obtained for Y(III), Nd(III), Dy(III) and Ce(IV). Then, 75.04% of Sc(III) can be precipitated from the organic by 2 M NaOH.

Chapter 4. Development of an REE Solvent Extraction Process using Synthetic AMD Pre-Concentrate Leachate

4.1. Introduction

In order to develop a solvent extraction process to recover REEs from the AMD pre-concentrate, the initial extraction tests were performed with a simulated leachate with five REEs discussed above and major elements including Al, Ca, Mg, Zn, Fe, Cu, Co, Ni and Mn. The elemental composition of the simulate leachate was designed similar to the concentrations in an actual AMD pre-concentrate, which was obtained by processing the AMD at Omega site by two-stage precipitation. The objective is to investigate the separation of REEs from the major elements and determine an optimal solvent extraction process to recover high purity MREO from the simulated leachate.

4.2 Methodology

4.2.1 Materials

(1) Synthetic simulated leachate

The desired concentration of the synthetic leachate was determined by assuming full dissolution of 136 grams of pre-concentrate in a 1L acid solution. By calculation, this dissolution procedure will produce a total concentration of the five surrogate REEs (i.e. Sc, Ce, Nd, Dy, and Y) of approximately 100 mg/L. The concentration of the five REEs and all the gangue metals ("Target") in the leachate is calculated and listed in Table 4.1. The simulated leachate is prepared according to the "target concentration". The actual concentrations of the simulated leachate were confirmed by ICP-MS (Table 4.1)

The simulated leachate was prepared by dissolving the calcium hydroxide ($Ca(OH)_2$) and metallic nitrates ($Al(NO_3)_3$, $Cu(NO_3)_2$, $Fe(NO_3)_3$, $Mg(NO_3)_2$, $Mn(NO_3)_2$, $Ni(NO_3)_2$ and $Zn(NO_3)_2$) in the deionized water. The resultant solution was then mixed with the standard solution of Co(III), Sc(III), Y(III), Nd(III), Dy(III) and Ce(IV).

Table 4.1 The target and actual concentrations of elements in simulated leachate

	Major Gangue Metals			Minor Gangue Metals						REEs				
mg/L	Al	Ca	Zn	Mg	Ni	Mn	Fe	Co	Cu	Sc	Ce	Nd	Dy	Y
Target	20883.4	861.2	507.1	173.0	146.9	114.6	80.4	52.7	17.4	20.0	24.0	20.2	0.1	41.0
Actual	19177.0	837.2	486.9	178.5	144.4	105.6	81.7	51.0	17.2	20.0	23.1	19.3	0.1	40.5

During the tests with the simulated leachate, notable precipitation occurred when the pH was adjusted to the target values of 2.0 and above. As a result, the initial solvent extraction experiments were conducted at pH 0.7, which was the original pH of the simulated leachate after preparation.

(2) Chemicals

In the present work, Di-(2-ethylhexyl) phosphoric acid (D2EHPA, 95%, Alfa Aesar, Haverhill, MA) and tri-n-butylphosphine (95%, Alfa Aesar, Haverhill, MA) were used as the extractant and modifier without further purification, respectively. The two solvents were dissolved in the Elixore 205 (supplied by Total Special Fluids, Inc. - Houston, TX).

Hydrochloric acid (HCl) was used as the stripping reagent and diluted using deionized water to obtain different concentrations. Hydroxylamine hydrochloride ($NH_3OH \cdot HCl$) was employed as the reductant, which was provided by Alfa Aesar (Haverhill, MA).

4.2.2 Experimental procedure

Studies have shown that the extraction ability of D2EHPA to Fe(II) is much poorer than that to Fe(III) (X. Li et al., 2011). Thus, reducing agents can be employed to reduce Fe(III) to Fe(II) before solvent extraction to decrease the amount of Fe entering the organic phase. Reduction experiments were carried out at room temperature. In each test, a certain amount of simulated leachate was mixed with different amount of reductant for a certain time. The concentrations of total iron and ferrous ion in simulated leachate were determined by ICP-MS and spectrophotometer (Hach, DR3900), respectively.

Solvent extraction experiments were performed in the separatory funnel at room temperature, using a mechanical shaker (Yamato, SA320). After extraction, the aqueous

phase was separated from the organic phase and diluted to rational multiples to analyze the concentrations of metals with ICP-MS. The organic phase was collected for the stripping tests.

As the organic phase could not be analyzed with ICP-MS directly, HNO_3 was used to digest the organics before analyzing. After digestion, the concentrations of metals in the loaded organic were determined with ICP-MS. Stripping experiments were conducted in the separatory funnel. In each test, the loaded organic was mixed with HCl solution with different concentrations and agitated by a shaker. After stripping, the organic phase was digested with HNO_3 and diluted prior to the ICP-MS analysis of metal concentrations. The concentrations of metals in the aqueous phase were calculated by mass balance.

4.3 Results and discussion

4.3.1 Solvent extraction behavior of elements in simulated leachate

The extraction behavior of REEs and major metals were studied using 0.2 M D2EHPA as the extractant and different concentrations of TBPO as the modifier, e.g., 0, 2.5 and 5 vol. % at a range of phase ratio (V_O/V_A) from 1:3 to 3:1.

Fig 4.1 and Table 4.2 shows the effects of phase ratio and TBPO concentration on the extraction efficiency of Al(III), Ca(II), Zn(II), Mg(II), Fe(III) and five REEs. The presence of TBPO helps the extraction of Al(III) and its extraction efficiency increases with the increase of TBPO concentration. In addition, the extraction efficiency of Al(III) increases with the increase of phase ratio (V_O/V_A) in the presence of TBPO; however, the extraction efficiency is not sensitive to phase ratio in solutions without TBPO. Likewise, the extraction efficiency of Zn increases with the increase of phase ratio (V_O/V_A), however, the TBPO has only little effect on its extraction. More than 30% extraction of Al(III) and Zn(II) is observed at the phase ratio (V_O/V_A) of 3:1 with TBPO concentration of 5 vol.%, which is detrimental to the REEs/Gangue metals separation. Since the total amount of Al(III) and Zn(II) is about 200 times as much as REEs, a slight increase in the extraction efficiency of Al(III) and Zn(II) will lead to large amount of Al(III) and Zn(II) entering organic phase with REEs. In addition, there is a slight increase in the extraction

efficiency of Ca(II) with the increase of phase ratio and TBPO concentration. However, the extraction efficiencies are no more than 15%.

Similar to Al(III), TBPO facilitates the extraction of Cu(II) greatly and its extraction efficiency increases with the increase of TBPO concentration. In addition, with 2.5 and 5 vol. % TBPO, a high phase ratio (V_O/V_A), also causes a sharp increase in the extraction efficiency of Cu(II), which can reach to 80% ~ 90%. The extraction efficiency of Fe(III) is more than 90% for all test conditions, which means that Fe(III) cannot be separated from REEs by solvent extraction.

Fig 4.1 also shows the extraction behavior of REEs under the same conditions. The total extraction efficiency of the five REEs increase with the increase of phase ratio (V_O/V_A). In addition, TBPO also significantly facilitates the extraction. The results are consistent with the discussion above.

Table 4.2 Extraction efficiency of elements in simulated leachate

V_O:V_A	Extraction, %									
	Al	Ca	Zn	Mg	Ni	Mn	Fe	Co	Cu	TREEs
c(TBPO) = 0 vol %										
1/3	3.2	0.7	10.0	2.7	0.0	0.0	92.9	0.0	6.9	67.9
1/2	2.8	1.0	11.5	2.7	0.0	0.0	95.2	0.0	4.3	71.8
1	2.6	3.4	17.1	7.0	0.1	0.0	97.0	0.0	11.9	77.8
2	2.2	7.2	22.6	4.7	0.1	0.0	97.6	0.0	5.2	86.8
3	3.1	6.1	32.5	7.0	0.2	0.0	97.2	0.0	7.6	89.7
c(TBPO) = 2.5 vol %										
1/3	4.7	2.0	1.3	1.9	0.0	0.0	94.6	0.0	4.3	83.9
1/2	6.0	5.0	10.5	6.6	0.0	0.0	97.5	0.0	16.4	90.8
1	8.8	6.7	16.9	10.6	0.0	0.1	97.8	0.0	31.1	96.0
2	13.6	7.4	17.9	8.1	0.1	1.1	98.1	0.0	47.3	98.3
3	15.9	9.6	30.2	9.9	0.2	0.0	98.1	0.0	89.2	99.7
c(TBPO) = 5 vol %										
1/3	4.7	1.8	6.7	4.4	0.0	0.0	97.1	0.0	20.5	88.7
1/2	7.5	4.9	11.4	6.9	0.0	0.0	97.6	0.0	33.8	94.8
1	14.5	6.5	19.0	12.3	0.1	0.0	98.3	0.0	76.3	97.3
2	20.7	10.5	22.9	11.7	0.1	0.0	99.1	0.0	103.6	99.1
3	31.6	11.2	32.5	9.8	0.2	0.0	99.1	0.0	99.8	99.2

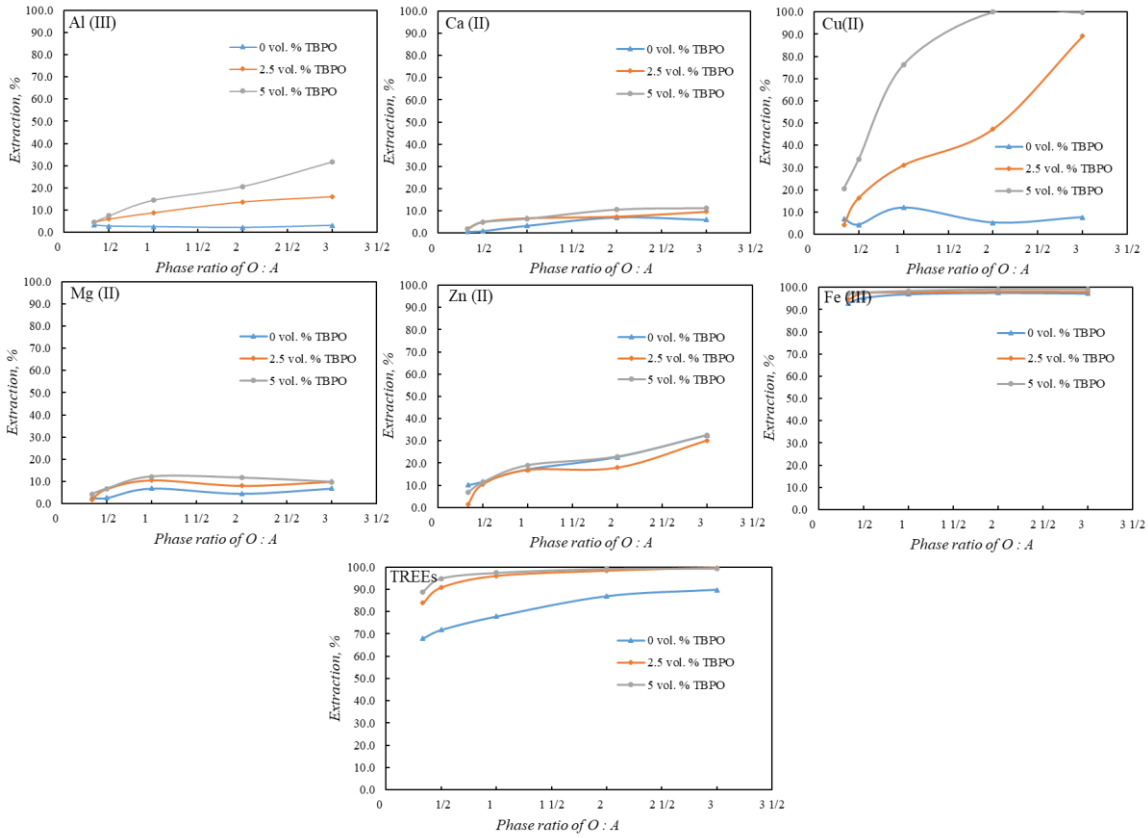

Fig 4.1 Extraction behavior of major elements and REEs in simulated leachate.

TREEs includes Sc(III), Y(III), Ce(IV), Nd(III) and Dy(III).

c(D2EHPA) = 0.2 M; pH = 0.7; t = 10 min.

Table 4.2 shows that the extraction efficiencies of Ni(II), Mn(II) and Co(II) are 0%, indicating that Ni(II), Mn(II) and Co(II) have been successfully separated from the REEs.

Overall, TBPO helps not only REE extraction, but also extractions of Al(III) and Cu(III). This is not good for the separation of REEs/gangue metals, especially for Al(III) removal. Fortunately, this problem can be solved by conducting solvent extraction at low phase ratio (V_O/V_A), since under this condition the extraction efficiencies of the gangue metals (except for Fe(III)) are much lower than those of REEs.

As shown in Table 4.3, when the TBPO concentration is 2.5 vol.% and the phase ratio (V_O/V_A) is 1:3, the extraction efficiencies of Al(III) and Cu(II) are less than 5% and the extraction efficiencies of Ca(II), Zn(II), Mg(II), Ni(II) and Co(II) are 0%. At the same

time, the extraction efficiency is more than 83.9% for TREEs. Although a large amount of gangue metals still enters the organic phase, the gangue metals except for Fe(III) can be removed by multi-staged solvent extraction due to the high selectivity of REEs over these metals (Table 4.3). The separation factor is calculated by the distribution coefficient of TREEs over that of the gangue metal, which is given by,

$$\alpha_{TREE/Gangue} = \frac{C_{org\_TREE} \times C_{Aqu\_gangue}}{C_{Aqu\_TREE} \times C_{org\_gangue}} \qquad 4.1$$

Where C_{org_TREE} and C_{org_gangue} represent the concentration of TREEs and gangue metal in organic phase, respectively. C_{Aqu_TREE} and C_{Aqu_gangue} represent the concentration of TREEs and gangue metal in aqueous phase, respectively.

Table 4.3 The results of solvent extraction test with 2.5 vol.% TBPO at phase ratio (V_O/V_A) of 1:3

	Al	Ca	Zn	Mg	Ni	Mn	Fe	Co	Cu	TREE
Extraction %	4.7	2.0	1.3	1.9	0	0	94.6	0	4.3	83.9
Con. in organic (mg/L)	1846	49.9	19.2	10.4	0	0	232	0	2.2	259.2
Separation factor	3770	4279	1647	6456	--	--	14	--	162	/

Therefore, it is necessary to conduct more research on the separation of Fe(III) and REEs. Studies have shown that the extraction ability of D2EHPA to Fe(II) is much poorer than that to Fe(III) (X. Li et al., 2011). Thus, reducing agents can be employed to reduce Fe(III) to Fe(II) before solvent extraction to decrease the amount of Fe entering the organic phase.

4.3.2 Pretreatment of simulated leachate by reduction

Hydroxylamine hydrochloride is one of the most effective reducing agents to reduce Fe(III) to Fe(II). The reduction reaction is shown below:

$$2NH_2OH + 4Fe^{3+} = 4Fe^{2+} + N_2O + 4H^+ \qquad 4.2$$

To determine the optimal reduction conditions for the simulated leachate, various experimental parameters, including reaction time and the dosage of reductant, were investigated.

(1) Reaction kinetics

The reaction kinetics were studied using 100 ml of simulated leachate and a stoichiometric amount of reductant, i.e., 0.15 ml of 0.5 M $NH_3OH \cdot HCl$. The reduction tests were conducted in the sealed tubes to isolate the oxygen from the solution. Fig 4.2 shows that the reduction efficiency of Fe(III) increases with the increase of reaction time. After 20 min, the reduction efficiency is close to 100%, indicating that the reduction of Fe(III) to Fe(II) was completed.

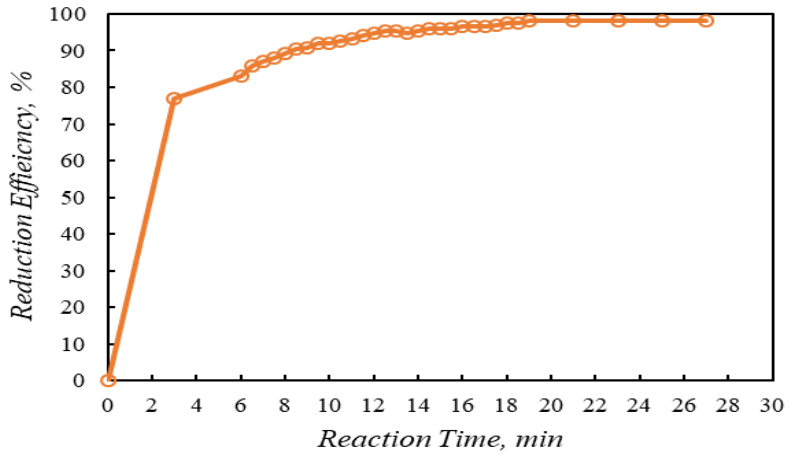

Fig 4.2 The effect of reaction time on the reduction efficiency of Fe

0.15 ml of 5 M $NH_3OH \cdot HCl$ per 100 ml simulated leachate in a sealed tube.

(2) The dosage of reductant

A series of experiments were also carried out at different dosages of reductant to determine the optimal reductant dosage. After reduction, the extraction behavior of Fe in solvent extraction was studied using 0.2 M D2EHPA + 0.25 vol.% TBPO at a phase ratio (V_O/V_A) of 1:3. Fig 4.3 shows that the extraction efficiency of Fe decreases with the increase of the reductant dosage. Without reduction, the extraction efficiency of Fe is 97.74%. At a stoichiometric dosage of reductant, there is only a slight decrease in the extraction efficiency, which indicates that the most of Fe(II) is oxidized to Fe(III) in solvent extraction. When the actual dosage is 40 times of stoichiometric dosage, the extraction efficiency of Fe decreases to 6.36%. At this condition, the presence of excess reductant help avoid the oxidation of Fe(II).

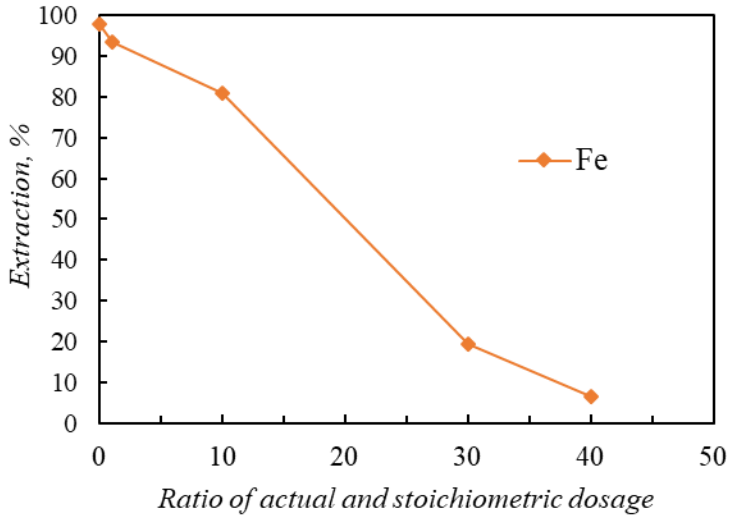

Fig 4.3 The effect of reductant dosage on the extraction efficiency of Fe

Reduction: T = 298 K; t = 20 min

Extraction: c(D2EHPA) = 0.2 M; c(TBPO)=2.5 vol.%; V_O/V_A=1:3; t = 10 min.

4.3.3 Stripping behavior of elements in simulated leachate

The stripping efficiency of each element was investigated by using different concentrations of HCl (0-6 M) at a phase ratio (V_O/V_A) of 1:1. The loaded organic phase was obtained from the reduction-solvent extraction process described above. The organic phase was digested with HNO_3 and diluted to analyze the concentrations of metals with ICP–MS. The results are listed in Table 4.4. Compared to the elements in simulated leachate (Table 4.1), Ni(II), Mn(II), Co(II) and Mg(II) have been removed through solvent extraction. The REEs, especially Y(III) has been enriched significantly. Al(III) is still the major contaminant.

Table 4.4 The concentrations of elements in the loaded organic phase

	Al	Ca	Fe	Cu	Zn	Sc	Y	Ce	Nd
Con. mg/L	647.9	54.2	85.8	22.1	23.5	59.7	122.7	15.4	17.1

Fig 4.4 shows the stripping behavior of gangue metals and REEs. The stripping efficiencies of five gangue metals increase with the increase of HCl concentrations and all REEs except for Sc(III) can be stripped with HCl, which is consistent with the previous studies. When the HCl concentration is 0, the stripping efficiencies of both

gangue metals and REEs are very low. It indicates that the gangue metals cannot be removed by stripping with water. When the HCl concentration is 0.1 M, 81.57% of Zn(II) and 40.48% Ca(II) are stripped to the aqueous phase while the REEs remain in the organic phase. Therefore, the removal of Zn(II) and Ca(II) may be achieved by using 0.1 M HCl. With the further increase of HCl concentration, the stripping efficiencies of REEs, especially Ce(III) and Nd(III) increase sharply and reach to nearly 100% at 6 M. At the same time, most of Fe(II), Cu(II) and Al(III) are stripped with REEs.

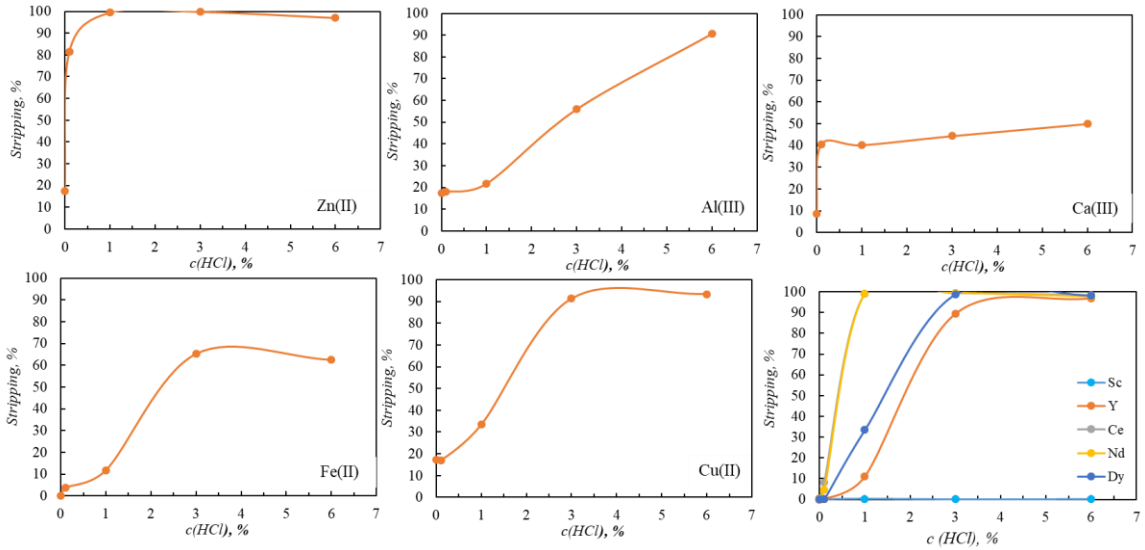

Fig 4.4 Stripping behavior of major elements and REEs in simulated leachate.

V_O/V_A=1:1; t = 10 min.

Based on the information above, the preliminary SX process developed for the recovery of REEs from simulated leachate was determined (Fig 4.5), which consists of the following major unit operations: (1) The reduction of Fe(III) to Fe(II) in simulated leachate; (2) Separation of REEs from gangue metals by solvent extraction with D2EHPA+TBPO; (3) Removal of Zn(II) and Ca(II) by scrubbing with 0.1 M HCl; (4) Stripping of REEs except for Sc with 6 M HCl. The optimal conditions in reduction and solvent extraction stages have been described in the previous sections. In addition, the effect of HCl concentration on the stripping efficiency of each element has also been fully investigated.

For a single stripping stage, the fraction of the desired component that can be recovered depends on the chemical conditions as well as the aqueous to organic phase

ratio. In addition, the phase ratio also affects the total concentration of REEs in strip liquor. With lower phase ratios (V_A:V_O), higher concentrations of REE can be achieved in the strip liquor but at the expense of lower recovery. The purpose of seeking a concentrated strip solution is to reduce the energy required to recover the product from the strip solution. In our case, precipitation will be used to generate the final product. The more concentrated the strip solution, the less energy is required to recover the desired components in the precipitation. Therefore, the phase ratio in the stripping was investigated to generate the strip liquor with both high recovery and concentration of REEs. Likewise, the phase ratio in the scrubbing stage was also studied to remove as much as gangue metals without the loss of REEs.

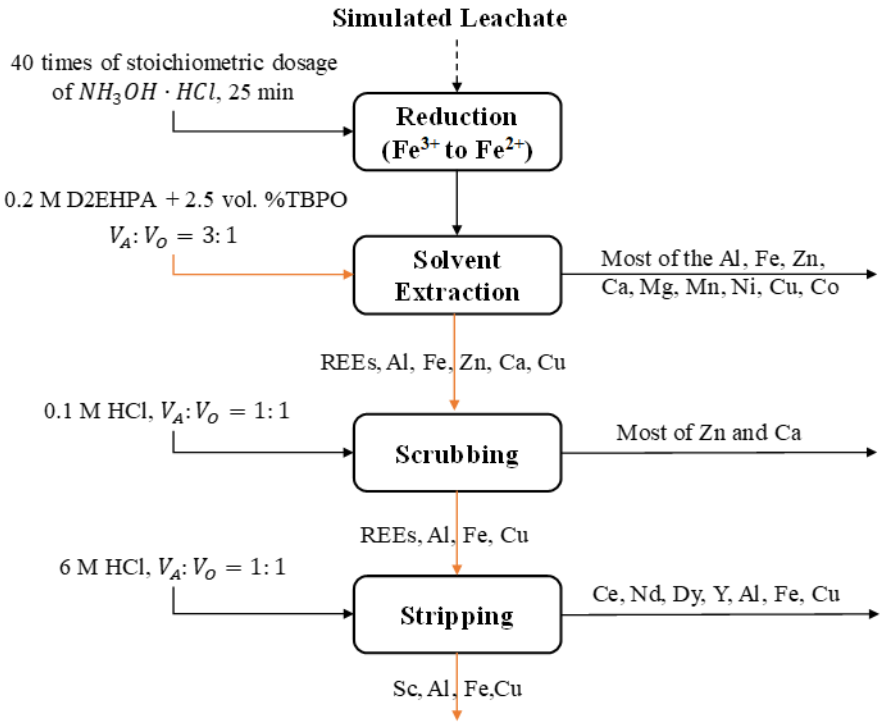

Fig 4.5 The preliminary SX process for the recovery of REEs from simulated leachate

Black lines: aqueous streams; Yellow lines: organic streams

4.3.4 The optimization of phase ratio in scrubbing and stripping stage.

(1) The effect of phase ratio on the scrubbing

The effect of phase ratio on the scrubbing of each element was investigated by using 0.1 M HCl at different phase ratios (V_A:V_O). The elemental composition of the

loaded organic feed was shown in Table 4.4. The previous study has indicated that Sc(III) cannot be stripped from D2EHPA with HCl at any conditions. Therefore, the results of Sc(III) will be omitted.

Fig 4.6 shows the scrubbing behavior of gangue metals. The scrubbing efficiency of Al(III) is close to 0% at all phase ratios. Since the amount of Al accounts for nearly 80% of the gangue metals, the scrubbing stage is not effective in the removal of impurities. However, it was found that a deleterious emulsion was formed when the loaded organic contacted the stripping reagent (6 M HCl) directly after solvent extraction. However, in cases where the loaded organic was first washed with water or diluted acid, no emulsion was formed in the stripping stage. Therefore, it is necessary to employ the scrubbing stage to help the phase separation in the process. Also, other gangue metals can be removed from organic with 0.1 M HCl, and their scrubbing efficiency increases with the phase ratio (V_A:V_O). In particular, around 80% of Zn(II) can be removed when the phase ratio is 1:1. When the phase ratio is larger than 1:1, the scrubbing efficiency of Zn(II) remains the same, and that of Ca(II) and Cu(II) increases. However, the scrubbing efficiency of Ce(IV) and Nd(III) also increases significantly, which reduces the recovery of REEs (Fig 3.7). Therefore, the optimal phase ratio (V_A:V_O) in scrubbing stage is set at 1:1, which represents an optimal tradeoff between gangue removal, REE recovery, and emulsion mitigation.

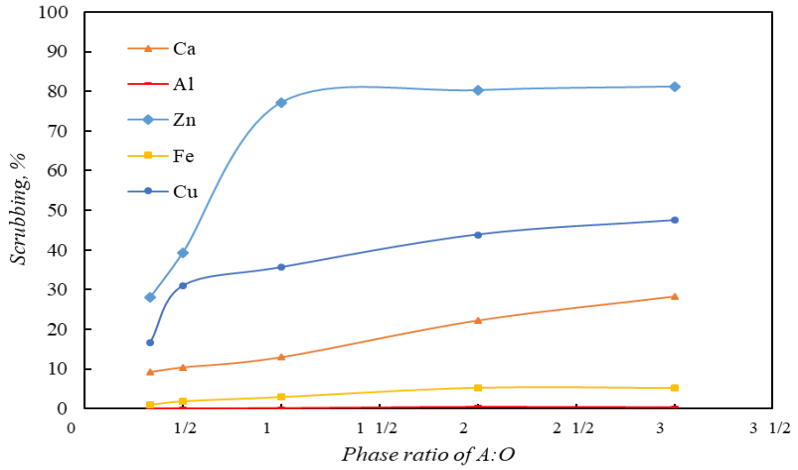

Fig 4.6 The effect of phase ratio on the scrubbing efficiency of gangue metals

c(HCl) = 0.1 M; t = 10 min.

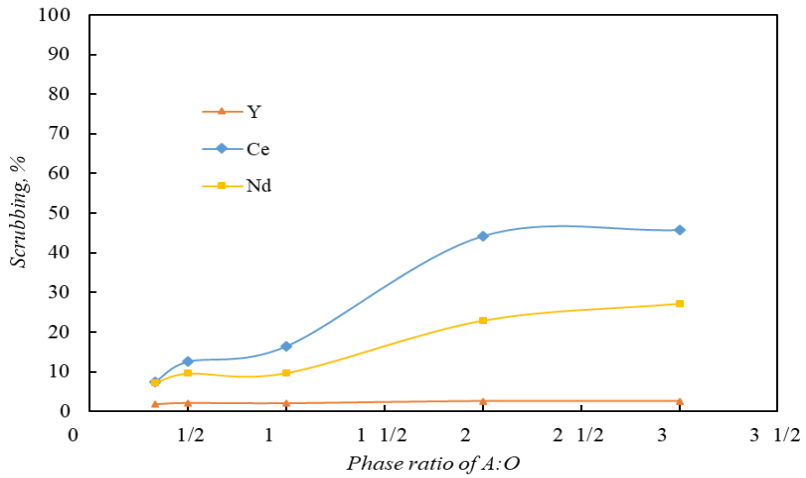

Fig 4.7 The effect of phase ratio on the scrubbing efficiency of REEs

c(HCl) = 0.1 M; t = 10 min.

(2) The effect of phase ratio on the stripping

The effect of phase ratio on the stripping of each element was investigated by using 6 M HCl at different phase ratio (V_A:V_O). The loaded organic was obtained from the optimal scrubbing process. Table 4.5 shows the elemental composition of the organic feed.

Table 4.5 The concentrations of elements in the organic feed for the stripping stage

	Al	Ca	Fe	Cu	Zn	Sc	Y	Ce	Nd
Con. mg/L	647.1	47.2	83.3	14.2	5.4	58.3	120.1	12.8	15.5

Fig 4.8 shows the stripping behavior of gangue metals and REEs at different phase ratios. The stripping efficiency of five gangue metals increases with the increase of phase ratio (V_A:V_O). Especially, the stripping efficiency of Al(III) increases from 14.7% to 90.6% when increasing the phase ratio (V_A:V_O) from 1:10 to 1:1. Since the Al(III) is the dominant contaminant, an increase in the stripping efficiency of Al(III) will lead to a large amount of Al(III) entering the strip liquor, which is detrimental to the subsequent purification of REEs. Likewise, the stripping of Fe(III) and Ca(II) is also very sensitive to the change of phase ratio. The stripping efficiency of Fe(III) and Ca(II) increases from 20.2% to 62.6% and from 10.3% to 50.0% respectively. Also, more than 90% of Cu(II) and Zn(II) can be stripped from organic when the phase ratio (V_A:V_O) is larger than 1:5.

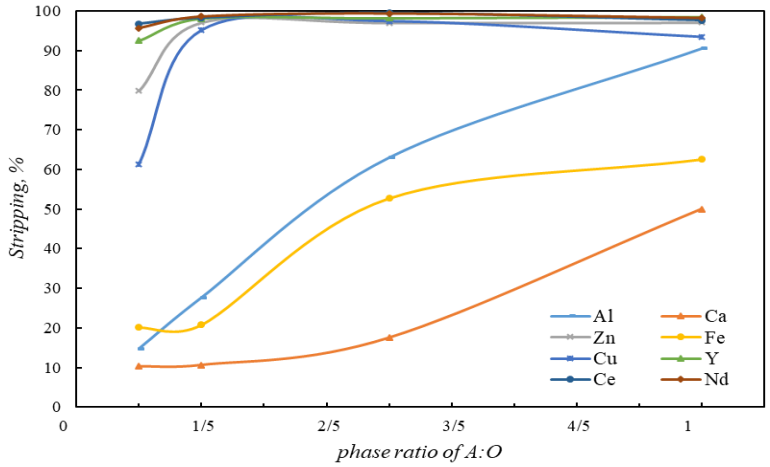

Fig 4.8 The effect of phase ratio on the stripping efficiency

c(HCl) = 6 M.; *t* = 10 min.

Concurrently, the stripping efficiency of Y(III), Ce(III) and Nd(III) remain nearly 100% at all phase ratios. Therefore, stripping at low phase ratio (V_A:V_O) will achieve both high recovery of REEs and high retention of gangue metals in the organic phase. Fig 4.9 shows the mass percentage (i.e. solution purity) of REEs in the strip liquor obtained at different ratios. As shown, the percentage of REEs increases with the decrease of phase ratio (V_A:V_O), which is optimal for the further purification of REEs. As a result, the optimal phase ratio (A:O) of stripping is set at 1:10.

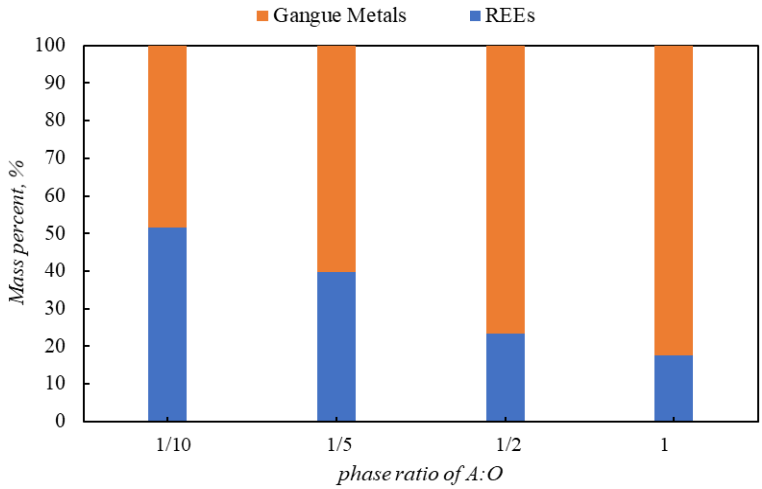

Fig 4.9 The effect of phase ratio on elemental composition of strip liquor

c(HCl) = 6 M; *t* = 10 min.

4.3.5 Optimal SX process for REE recovery from simulated leachate

The SX process for the recovery of REEs from simulated leachate was optimized (Fig 4.10), where the optimal phase ratio (V_A:V_O) in scrubbing and stripping stages is set at 1:1 and 1:10 respectively. Fig 4.10 also shows the elemental composition of each stream in the process. The REEs except for Sc(III) are enriched throughout the process. The total amount of four REEs (Y, Ce, Nd, and Dy) accounts for only 0.37% in simulated leachate and increases significantly to 50.30% in the strip liquor. Correspondingly, the amount of Al(III) decreases from 91.59% to 36.44% through the process.

Table 4.6 compares the element concentration in the simulated leachate and the strip liquor. 99.8% of the gangue metals are removed through the process. The removal rate of Al(III) is almost 99%; however, Al(III) is still the primary contaminant in the strip liquor because of its high concentration in the original leachate. In addition, the strip liquor also contains trace amounts of Cu(II), Fe(III), Ca(II) and Zn(II); however, the concentration of these elements is much lower than that of REEs. Furthermore, all of the Mg(II), Ni(II), Mn(II), and Co(II) are removed by the process.

Table 4.6 Comparison of the elemental composition of simulated leachate (SL) and strip liquor

	SL	Strip liquor	Removal		SL	Strip liquor	Recovery
	mg/L	mg/L	%		mg/L	mg/L	%
Al	20840.9	952.2	99.8	Sc	20.4	0.0	0.0
Ca	756.6	48.3	99.8	Ce	23.6	124.2	17.6
Zn	485.1	42.8	99.7	Nd	20.2	147.9	24.4
Mg	169.8	0.0	100.0	Dy	0.12	0.0	0.0
Ni	138.1	0.0	100.0	Y	40.6	1110.7	91.2
Mn	108.6	0.0	100.0	Total	104.9	1383.0	44.0
Fe	80.0	167.9	93.0				
Co	53.7	0.0	100.0				
Cu	15.7	87.2	81.5				
Total	22648.6	1298.5	99.8				

In total, 44.0% of REEs are recovered to the strip liquor, and the total concentration of REEs in the strip liquor is more than ten times of that in the simulated leachate. Notably, 91.2% of Y(III) is recovered, and a high concentration of 1110.7 mg/L was produced in the strip liquor. Alternatively, Ce(IV) and Nd(III) had much lower

recoveries, 17.6% and 24.4%, respectively. Ce(IV) and Nd(III) are lost in the initial extraction step given the low extraction rates of light REEs at low pH and low phase ratio (V_A:V_O) in D2EHPA. Sc(III) cannot be stripped with HCl and remains in the loaded organic. Following this process, the strip liquor with concentrated REEs will be sent to the precipitation stage for the generation of REE oxide products.

REE oxalate was precipitated from the strip liquor initially generated from the simulated leachate. The oxalate was then converted to oxide by calcination. Fig 4.11 shows the compositions of the final REE oxide. As shown, the total rare earth oxide content is 92.8%, of which 89.6% is Yttrium. The results show the feasibility of generating high grade REE oxide from simulated leachate by the optimal SX process.

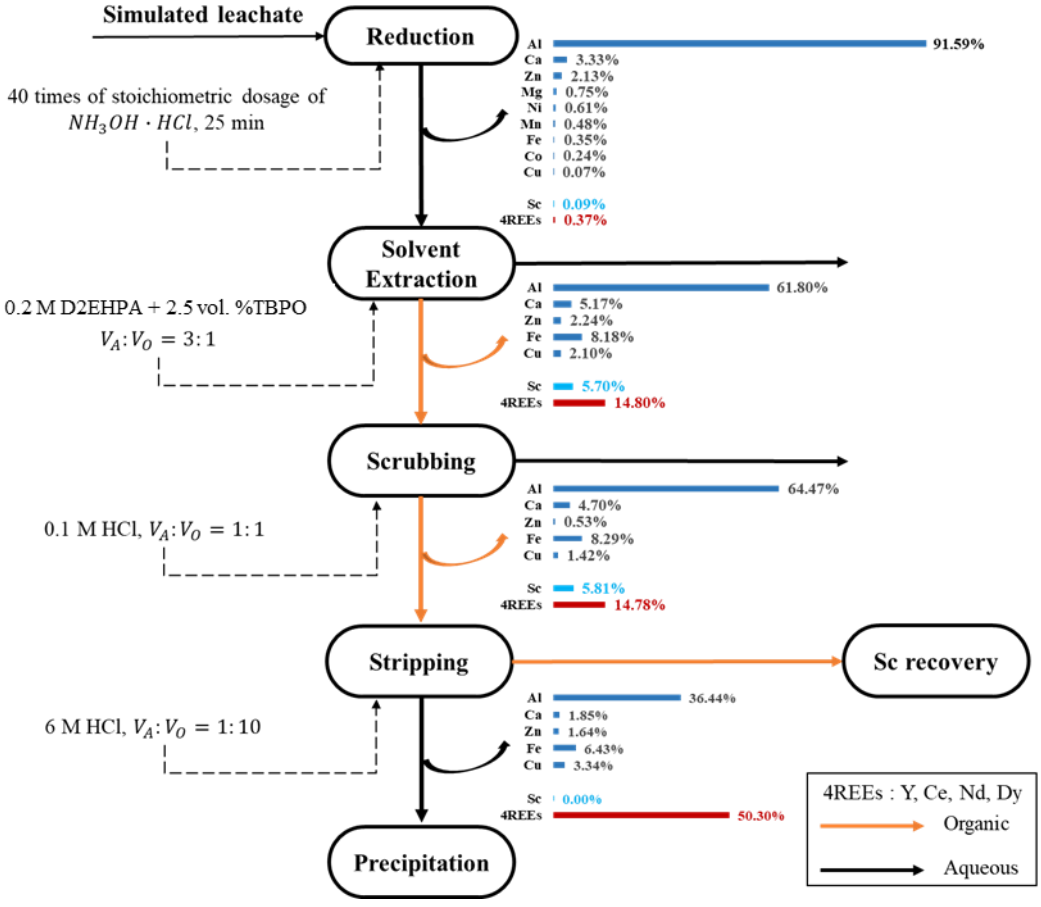

Fig 4.10 The flowsheet and elemental composition of each stream of the optimized SX process

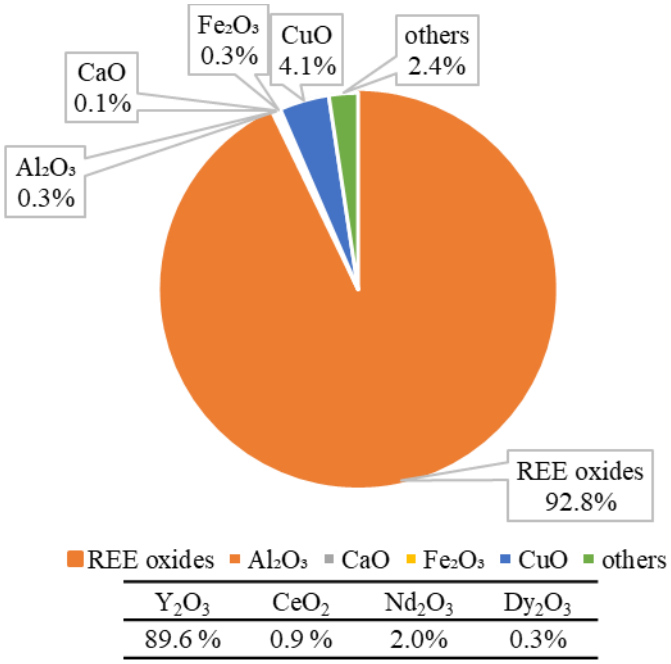

Y_2O_3	CeO_2	Nd_2O_3	Dy_2O_3
89.6 %	0.9 %	2.0%	0.3%

Fig 4.11 Compositions of REO product generated from simulated leachate

4.4 Conclusions

This chapter investigated the separation of REEs from the major elements including Al, Ca, Mg, Zn, Fe, Cu, Co, Ni and Mn through the experiments on simulated leachate. An optimal SX process to recover high purity MREO from the simulated leachate were developed, which is shown in Fig 4.10. Through the process, a rare earth oxide with 92.8% purity were obtained, of which 89.6% is Yttrium. Additional findings presented in this chapter include:

(1) Reduction of Fe(III) to Fe(II) helps inhibit a large amount of Fe being extracted with REEs. The extraction efficiency of Fe decreases from 97.74% to 6.36% by reduction.

(2) D2EHPA is able to selectively extract the REEs at low concentrations (100 mg/L) in the presence of a large amount of major elements (>20 g/L).

(3) Stripping at low phase ratio (V_A:V_O) will achieve both high recovery of REEs and high retention of gangue metals in the organic phase.

Chapter 5. Validation of an Optimal Solvent Extraction Process using Real Leachate derived from AMD Pre-Concentrate

5.1 Introduction

In a parallel study, REE pre-concentrate was generated using a pilot-scale mobile plant during the late spring and early summer of 2019 by Ziemkiewicz's research group in WVU. This pre-concentrate assayed approximately 0.1% REE, which is notably lower than the values expected from laboratory testing but similar in distribution of metals and REEs (unpublished). These pre-concentrate materials were later delivered to Virginia Tech and subsequently used as feedstock for the laboratory-scale solvent extraction tests to validate the optimal solvent extraction process derived from simulated leachate. The objective of the work in this chapter was to assess the capability of the SX process to recover high-grade MREO, exceeding 90% purity, from the pre-concentrate generated from AMD.

5.2 Methodology

5.2.1 Materials

(1) REE pre-concentrate

The REE pre-concentrate used as feedstock for the solvent extraction tests conducted in this chapter contained an average moisture content of 79.6% and a TREEs content of 0.13%. Table 5.1 shows the element composition of the dry concentrate.

5.2.2 Chemicals

In the present work, Di-(2-ethylhexyl) phosphoric acid (D2EHPA, 95%, Alfa Aesar, Haverhill, MA) and Tri-n-butylphosphine (95%, Alfa Aesar, Haverhill, MA) were used as the extractant and modifier without further purification, respectively. The two solvents were dissolved in the Elixore 205 (supplied by Total Special Fluids, Inc. - Houston, TX).

Hydrochloric acid (HCl) was used as the reagent in the scrubbing and stripping tests and diluted using deionized water to obtain different concentrations. Hydroxylamine hydrochloride ($NH_3OH \cdot HCl$) was employed as the reductant and oxalic acid ($C_2H_2O_4$) was used to selectively precipitate REEs, both of which were provided by Alfa Aesar (Haverhill, MA).

Table 5.1 Element composition of the dry REE concentrate

REEs	Concentration		MM	Concentration	
Sc	101.8	mg/kg	Al	303.2	g/kg
Y	364.4	mg/kg	Ca	26.2	g/kg
La	71.6	mg/kg	Co	0.6	g/kg
Ce	253.4	mg/kg	Fe	21.8	g/kg
Pr	38.5	mg/kg	Mg	4.1	g/kg
Nd	180.4	mg/kg	Mn	3.0	g/kg
Sm	53.2	mg/kg	Na	1.2	g/kg
Eu	14.1	mg/kg	Si	102.8	g/kg
Gd	82.6	mg/kg	SO4	1.4	g/kg
Tb	15.1	mg/kg	Cl	0.0	g/kg
Dy	88.5	mg/kg	Total	464.4	g/kg
Ho	17.1	mg/kg			
Er	46.7	mg/kg			
Tm	6.4	mg/kg			
Yb	36.1	mg/kg			
Lu	5.5	mg/kg			
Total	1,375.4	mg/kg			

5.2.3 Experimental procedure

(1) Acid leaching

Initially, 481.5 g of the REE pre-concentrate was mixed with 550 ml DI water in a beaker. Afterwards, 150 ml concentrated nitric acid was added to the beaker in 30 incremental steps to ensure the leaching process was carried out at pH = 1. After 5 hours, the insoluble residue was filtered and a brown filtrate with a pH =1 was obtained (Fig 5.1 (a)). The metal content of filtrate was measured by ICP-MS. The filtrate is denoted as “pregnant leach solution (PLS)” in the following discussion.

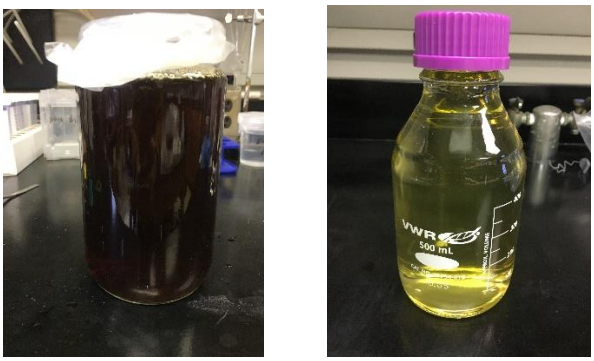

(a) (b)

Fig 5.1 The photo of pregnant leach solution (a) and leachate (b)

(2) Iron removal

In order to remove the iron that largely present in the PLS, 1 M NaOH solution was slowly added to the PLS to bring the pH up to around 3, where the formation of $Fe(OH)_3$ was observed. The solution was stirred for 5 minutes, left to rest for half an hour and then filtered. The resulting filtrate was a light yellow color and its metal content was analyzed by ICP-MS (Fig 5.1(b)). This filtrate is denoted as “leachate” in the following discussion.

(3) SX process

Solvent extraction experiments were performed in the separatory funnel at room temperature, using a mechanical shaker (Yamato, SA320). After extraction, the aqueous phase was separated from the organic phase and diluted to rational multiples to analyze the concentrations of metals with ICP-MS. The organic phase was collected for the scrubbing tests.

As the organic phase could not be analyzed with ICP-MS directly, HNO_3 was used to digest the organics before analyzing. After digestion, the concentrations of metals in the loaded organic were determined with ICP-MS.

Scrubbing and stripping experiments were conducted in the separatory funnel. In each test, the loaded organic was mixed with 0.1 M or 6 M HCl solution and agitated by a shaker for 10 min. After achieving equilibrium, the aqueous phase was separated from the organic phase and collected for the precipitation tests.

(4) The generation of REE oxide

Precipitation experiments were conducted in a 100 ml beaker at room temperature. The mixed REEs were precipitated from the strip liquor by oxalic acid. For each test, 2 g oxalic acid was added in 100 ml strip liquor, followed by the addition of the 1 M NaOH solution until a pH of 2.5 was reached. The mixture was stirred for half an hour and left to rest for 12 hours. Afterwards, the precipitated REE oxalate was filtered, washed with water, and dried at 60^{o} C. The oxalate was subsequently calcined in a muffle furnace at 800^{o}C for 5 h to convert it to an REE oxide product. The REE oxide was later washed with 2% nitric acid and dried at 60^{o} C. The purity of the final product was determined after subsequent dissolution in HCl and analysis of the solution with ICP-MS.

5.3 Results and Discussion

5.3.1 The composition of the pregnant leach solution (PLS)

Previous research has confirmed that nitric acid is the most suitable and reliable leaching reagent for acid mine drainage precipitates (AMDp) (Saber, 2016). In addition, pilot-scale tests conducted in a separate DOE study (DE-FE0026927) have shown that the PLS tends to form a pernicious alumino-silicate gel when the leaching tests are carried out at pH < 1, As a result, nitric acid was employed as the reagent, and the leaching tests were conducted at pH = 1, which represents an optimal tradeoff between leaching efficiency and operability.

Table 5.2 shows the element composition of the PLS generated from this process. It can be seen that the concentration of REEs is 90.7 mg/L. Among them, Y, Ce and Nd are present at a notable concentration of 25.0 mg/L, 16.3 mg/L and 12.6 mg/L, respectively. Most of the other REEs are also present at a concentration ranging from around 1 mg/L to 5 mg/L. The PLS is, therefore, a proven source of producing REEs product.

The total concentration of major elements is 26,796.3 mg/L, among which Al accounts for more than 60% with a concentration of 16,271 mg/L. Other notable constituents include Ca, Fe and Si with a concentration of more than 1000 mg/L. Minor constituents include Mg, Mn and Co of which the concentration is less than 500 mg/L.

The ratio of the major elements to REEs as well as the distribution of REEs in the real PLS is similar to that of the simulated leachate. This result suggests that the process knowledge and data generated from the simulated leachate testing has direct relevance to the real system evaluation.

Two notable exception, however, are that the concentration of Fe (1,307.1 mg/L) and Si (6,855.6 mg/L) are both higher than the values used in the simulated leachate. With regard to Fe, prior test work has shown that the Fe in the PLS must be reduced from Fe(III) to Fe(II) to prevent extraction into the organic phase (Fe(II) has a much lower extraction efficiency that Fe(III). Given the relatively high concentration of Fe in the real PLS, this approach was deemed infeasible, owing to the high reagent consumption and high cost needed to fully reduce all of the Fe. As an alternative approach, the Fe was instead removed from PLS by precipitating as iron hydroxide ($Fe(OH)_3$) at pH 3.

Table 5.2 Elemental composition of the PLS

REE	Concentration		MM	Concentration	
Sc	6.0	mg/L	Al	16271.0	mg/L
Y	25.0	mg/L	Ca	1825.5	mg/L
La	4.6	mg/L	Co	42.9	mg/L
Ce	16.3	mg/L	Fe	1307.1	mg/L
Pr	2.5	mg/L	Mg	251.6	mg/L
Nd	12.6	mg/L	Mn	140.4	mg/L
Sm	3.7	mg/L	Si	6855.6	mg/L
Eu	0.9	mg/L	Total	26796.3	mg/L
Gd	5.3	mg/L			
Tb	1.0	mg/L			
Dy	5.8	mg/L			
Ho	1.1	mg/L			
Er	3.1	mg/L			
Tm	0.4	mg/L			
Yb	2.4	mg/L			
Lu	0.3	mg/L			
Total	90.3	mg/L			

5.3.2 Fe removal by selectively precipitation

The PLS was processed to remove Fe by selectively precipitation. Fig 5.2 shows the recovery of each element in this process (i.e. the amount that remained in the solution after precipitation). It can be seen that more than 90% of Fe and Si were removed, which was due to that the rapid hydrolysis of Fe(III) at pH 3 resulted in precipitation of $Fe(OH)_3$. At the same time, $Fe(OH)_3$ provided a surface area for silicate absorption and thus a rapid Fe/Si co-precipitation (Dyer et al, 2010). However, most of the other major elements remained in the solution during the precipitation process. Therefore, the recovery of total major elements is 78%.

For REEs, the total recovery is 91% which indicates a good separation efficiency between REEs and Fe/Si. The major loss of REEs is from Sc. As shown in Fig 5.2, 70% of Sc reported to the precipitate. Previous test work has shown that an additional stripping stage is necessary for the recovery of Sc as it cannot be stripped by acid with the other REEs. It has also been proven practical that Sc can be recovered from organic phase by the formation of $Sc(OH)_3$ precipitate. However, this method is time-consuming and involves a three-phase separation, which will make the recycle of solvent very difficult in future continuous production. Therefore, it will be more adequate for process development if all Sc can precipitate with Fe before solvent extraction. Future efforts should be conducted to explore the possibility of this method.

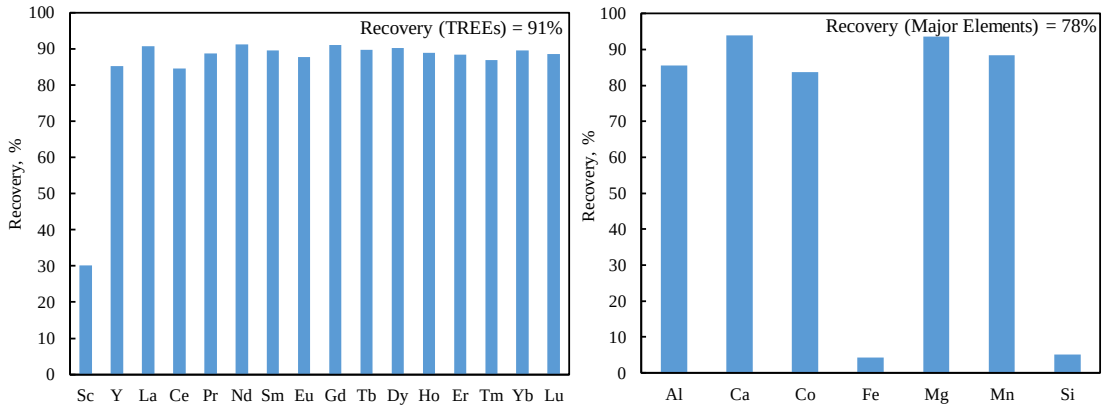

Fig 5.2 Recovery of REEs and gangue metals in selectively precipitation

Table 5.3 Elemental composition of the leachate

	Concentration			Concentration	
Sc	2.5	mg/L	Al	14094.6	mg/L
Y	23.3	mg/L	Ca	1721.3	mg/L
La	4.2	mg/L	Co	39.7	mg/L
Ce	14.7	mg/L	Fe	79.1	mg/L
Pr	2.2	mg/L	Mg	235.7	mg/L
Nd	11.5	mg/L	Mn	127.2	mg/L
Sm	3.4	mg/L	Si	118.9	mg/L
Eu	0.9	mg/L	Total	16416.5	mg/L
Gd	4.9	mg/L			
Tb	0.9	mg/L			
Dy	5.4	mg/L			
Ho	1.1	mg/L			
Er	2.8	mg/L			
Tm	0.4	mg/L			
Yb	2.2	mg/L			
Lu	0.3	mg/L			
Total	80.8	mg/L			

Table 5.3 shows the element composition of the leachate after Fe precipitation. Compared to the PLS, the leachate is more similar to the simulated leachate used in model system evaluation as the most of Fe and Si has been removed. Next, the leachate was processed with the optimal SX process shown in Chapter 3.

5.3.3 SX process

Preliminary tests on leachate showed insufficient extraction of LREEs with 0.2 M D2EHPA. To solve this problem, 0.5 M D2EHPA was used in the solvent extraction of the pre-concentrate. All the other conditions followed the optimal SX process described in Fig 4.10.

Fig 5.4 and Table 5.5 shows the concentrations of each element in the organic after extraction and scrubbing as well as the strip liquor obtained from the stripping. After extraction, there is a significant decrease in the concentration of Al and Ca and all of the Co, Mg, Mn were not extracted. Even though there is only a slight decrease in the concentration of Fe and even a slight increase in the concentration of Si, they will not lead to significant contamination as the majority of their mass was removed in the earlier

stage by precipitation. The concentration of REEs is almost doubled after solvent extraction, which indicates good separation efficiency between REEs and major elements in solvent extraction.

There is not much difference in the cocnentration of elements in the loaded organic during scrubbing stage. Previous test work showed that a deleterious emulsion was formed when the loaded organic contacted the stripping reagent (6 M HCl) directly after solvent extraction. However, in cases where the loaded organic was first washed with water or diluted acid, no emulsion was formed in the stripping stage. Therefore, scrubbing stage is still necessary for the process.

After stripping, REEs were further enriched with the concentration increasing from 161.9 mg/L in loaded organic to 466.8 mg/L in strip liquor. Most of the major gangue metals, Al and Ca, are removed. The concentration of Fe is notable, however, its concentration is lower than that of REEs.

Overall, the REEs are significantly concentrated through SX process, and the total concentration increases from 80.8 mg/L to 466.8 mg/L. Al is still the primary contaminant in the strip liquor because of its high concentration in the original leachate. Fe is also major contaminant because of its high recovery in extraction and stripping stages. In addition, the strip liquor also contains small amounts of Ca and Si. Furthermore, all of the Mg, Mn, and Co are removed by the process.

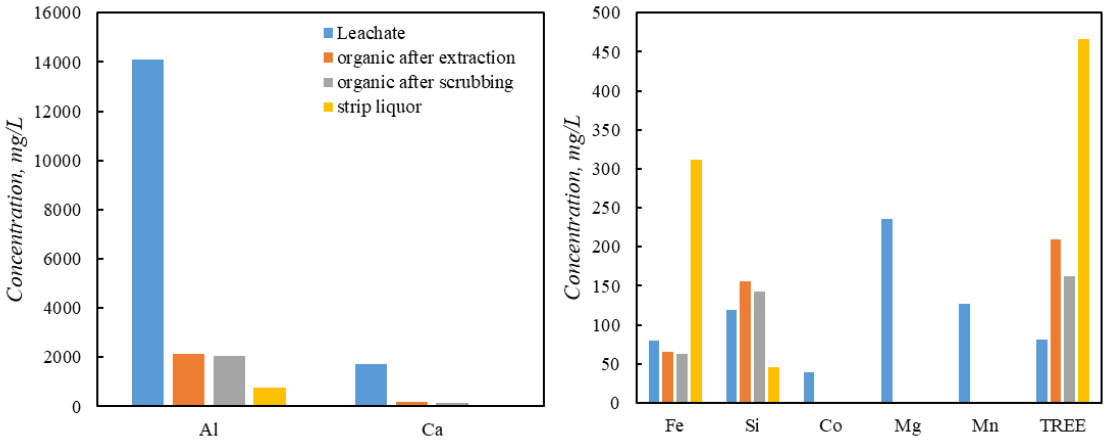

Fig 5.3 Concentration of the elements in the product of each stage in SX process

Table 5.4 Concentration of the elements in the product of each stage in SX process

REEs	Feed	Extraction	Scrubbing	Stripping	Gangue	Feed	Extraction	Scrubbing	Stripping
mg/L	Leachate	Loaded organic	Loaded organic	Strip Liquor	mg/L	Leachate	Loaded organic	Loaded organic	Strip Liquor
Sc	2.5	7.4	7.1	0.0	Al	14094.6	2120.8	2054.5	775.2
Y	23.3	72.9	70.0	107.4	Ca	1721.3	182.1	143.8	66.2
La	4.2	3.2	0.3	2.7	Co	39.7	0	0	0
Ce	14.7	25.7	6.3	42.4	Fe	79.1	65.8	62.7	311.5
Pr	2.2	4.7	1.6	10.3	Mg	235.7	0	0	0
Nd	11.5	26.0	11.0	68.0	Mn	127.2	0	0	0
Sm	3.4	9.5	8.5	46.0	Si	118.9	156.0	143.2	46.0
Eu	0.9	2.5	2.4	12.8	Total	16416.5	2524.8	2404.2	1207.1
Gd	4.9	14.6	13.6	73.6					
Tb	0.9	2.8	2.7	13.7					
Dy	5.4	17.8	17.4	65.7					
Ho	1.1	3.3	3.2	8.5					
Er	2.8	9.0	8.8	12.2					
Tm	0.4	1.2	1.2	0.7					
Yb	2.2	7.2	6.9	2.4					
Lu	0.3	1.0	1.0	0.3					
Total	80.8	208.9	161.9	466.8					

5.3.4 Recovery of REE oxalate

The precipitation of REE oxalate is widely used in industry for the selective recovery of rare earth metals (Xie et al., 2014). However, this method is usually applied to the leachate with enriched REEs (1-40 g/L) and limited impurities (Josso et al., 2018). The challenge lies in the low REEs concentration (0.5 g/L) and high concentration of impurities (1.2 g/L) in the strip liquor.

The tests were conducted by the addition of excess oxalic acid and precipitation at pH 2.5. Fig 5.4 shows the precipitation efficiency of each element. As shown in the plot, 88.5% of REEs was precipitated, while most of the major elements remained in the solution. In addition, the precipitation efficiency of the LREE is higher than that of the HREE, which is due to that the affinity for oxalate ligand decreases gradually from LREE to HREE at pH >2.3 (Josso et al., 2018). Among the major element, most of the Al, Fe, Si were removed but more than 80% of Ca precipitated with REEs. Fortunately, Ca can be removed by acid washing in the subsequent process.

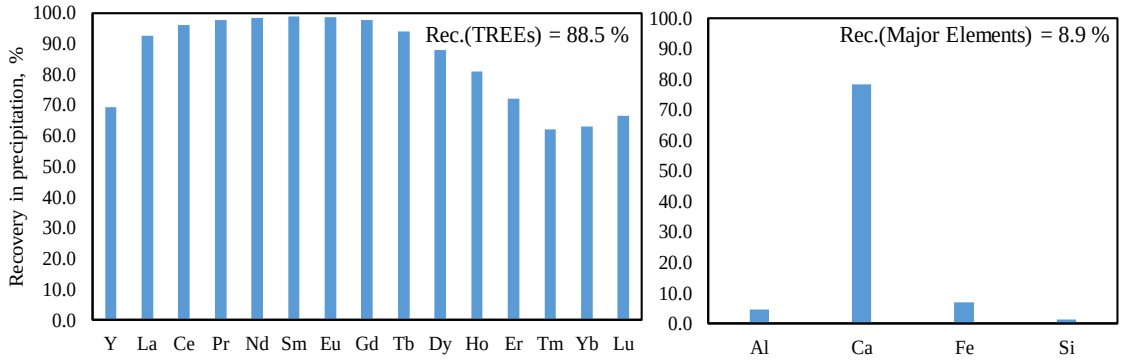

Fig 5.4 Recovery of REEs and in precipitation by oxalic acid

5.3.5 Recovery of REE oxide

The REE oxalate was oxidized by heating at 800°C for 5 h to obtain REE oxide. The REE oxide was then washed by 2% nitric acid to remove the soluble impurities, like Ca and Na. The distribution of the individual REE in the mixed oxide is given in Table 5.5 along with the mass fraction of each major element. As shown, the final product contains 90.5% TREO and 9.5% impurities. In addition, Y, Ce, Nd, Gd and Dy are enriched in the TREO with mass fractions over 10%.

Table 5.5 Compositions of REO product from pre-concentrate of AMD

Oxides	Concentration		Oxides	Concentration	
Y	20.8	%	Al	4.0	%
La	0.4	%	Ca	1.8	%
Ce	14.9	%	Co	1.0	%
Pr	2.1	%	Fe	1.9	%
Nd	11.6	%	Mg	0.2	%
Sm	8.4	%	Mn	0.1	%
Eu	2.3	%	others	0.7	%
Gd	13.2	%	Total	9.5	%
Tb	2.7	%			
Dy	10.6	%			
Ho	1.3	%			
Er	1.7	%			
Tm	0.1	%			
Yb	0.3	%			
Lu	0.0	%			
Total	90.5	%			

5.3.6 McCabe-Thiele diagrams for extraction and stripping stages

The McCabe-Thiele diagram is constructed for the extraction to find out the theoretical number of extraction stages and the extent of enrichment of TREEs in the loaded organic. From Figure 5.5, it can be seen that all REEs in the leachate can be extracted to organic phase in three counter-current extraction stages at a phase ratio (V_A:V_O) of 3:1 with 0.5 M D2EHPA + 2.5 vol.% TBPO. The loaded organic reads to contain around 250 mg/L of TREEs.

The McCabe Thiele diagram is also constructed for the stripping stage. Figure 5.6 shows that all the REEs in the loaded organic is able to be recovered to the strip liquor in two counter current stripping stages at a phase ratio of (V_O:V_A) of 1:1 with 6 M HCl. At this condition, the concentration of TREEs reads to 160 mg/L.

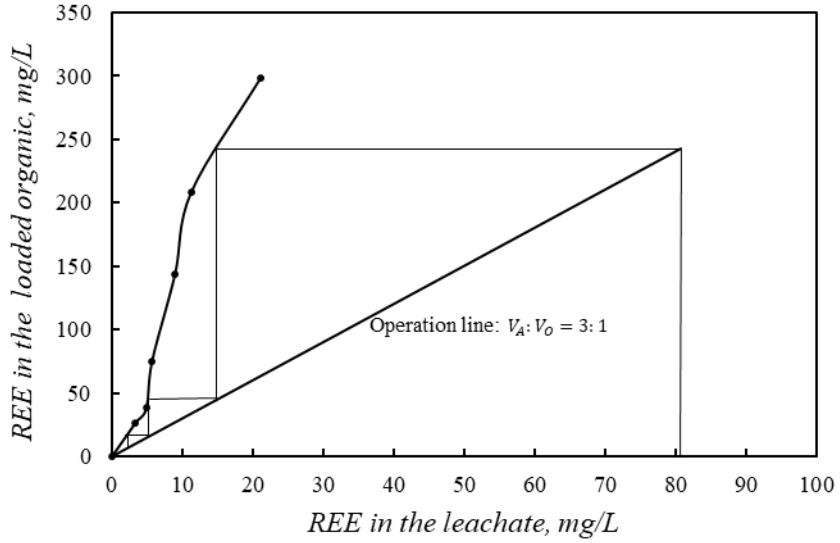

Fig 5.5 McCabe-Thiele diagram of extraction of TREE from leachate

c(D2EHPA) = 0.5 M; c(TBPO) = 2.5 vol. %, pH = 3.

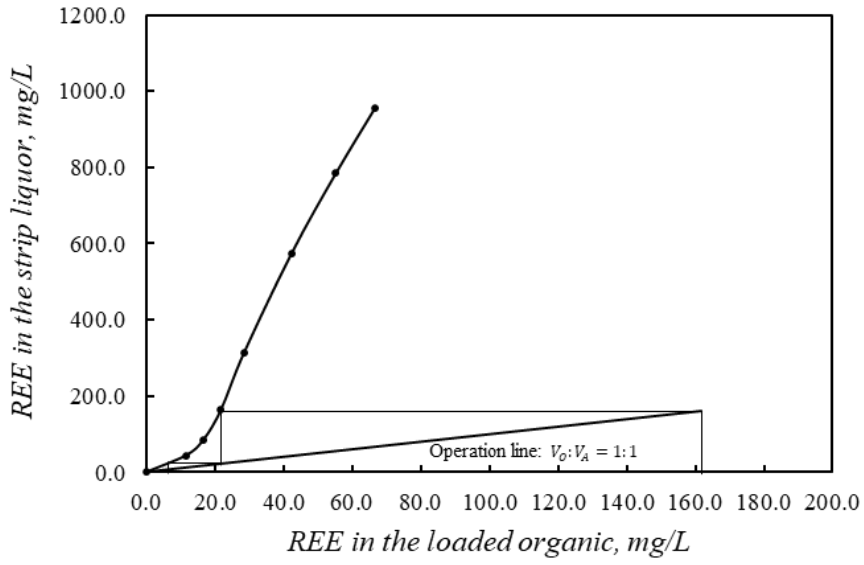

Fig 5.6 McCabe-Thiele diagram of stripping of TREE from loaded organic

c(HCl) = 6 M.

5.4 Conclusions

This chapter developed a process for REE recovery from AMD pre-concentrate of AMD based on the optimal solvent extraction process derived from simulated leachate, which is shown in Fig 4.7. The AMD pre-concentrate is first dissolved in the nitric acid. The resultant PLS is precipitated at pH 3 for Fe removal and the optimal SX process is then followed. After SX separation, the strip liquor is precipitated using oxalic acid and finally roasted to produce an REE oxide product. An oxide containing 90.5% REE was obtained from AMD pre-concentrate (0.1% REE) by this process.

The McCabe-Thiele diagrams were also constructed for the extraction and stripping stages. The diagrams show that theoretically the REEs in leachate can be operationally extracted in three counter-current extraction stages at a phase ratio (V_A:V_O) of 3:1 with 0.5 M D2EHPA + 2.5 vol.% TBPO and all the REEs in the loaded organic is able to be recovered to the strip liquor in two counter current stripping stages at a phase ratio of (V_O:V_A) of 1:1 with 6 M HCl.

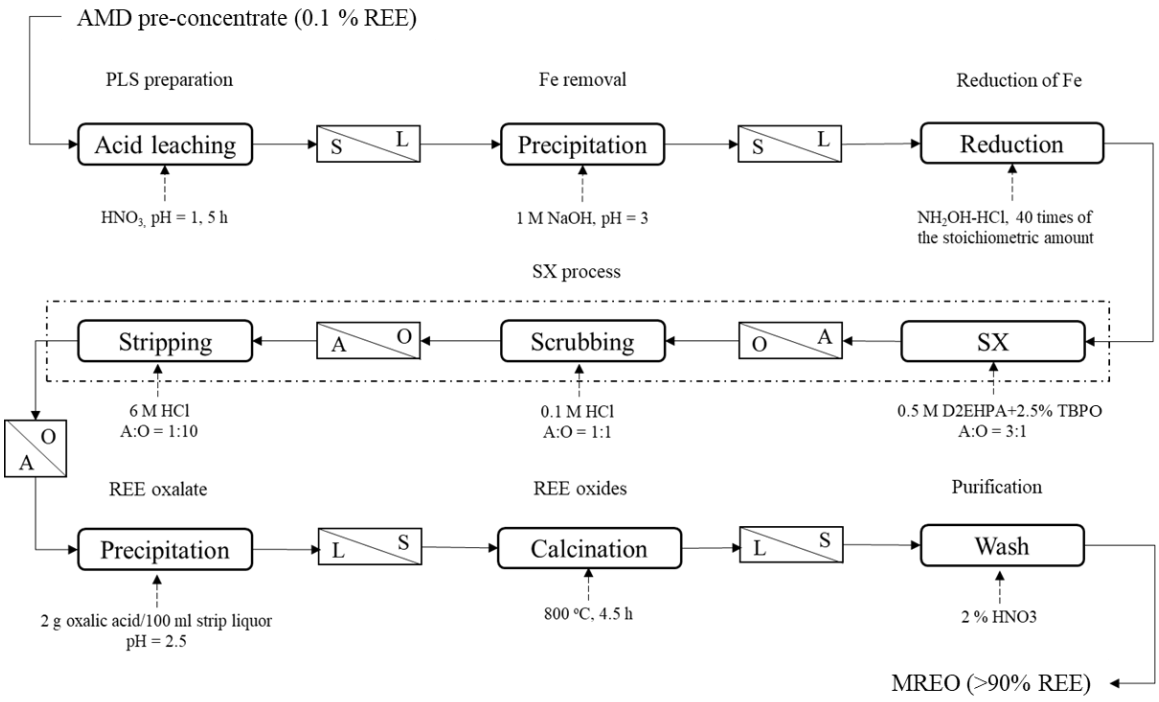

Fig 5.7 Flowsheet of the recovery of MREO from pre-concentrate of AMD

Chapter 6. Conclusions and Recommendations

The main objective of this study is to develop and optimize a laboratory-scale capable of producing mixed rare earth concentrates with purities exceeding 90% from an AMD pre-concentrate. In order to fulfill the objective, laboratory-scale batch solvent extraction tests were performed on synthetic REE solutions to determine the influence of various process parameters (e.g. pH, extractant dosage, diluent type, O:A ratio, and feedstock concentration). Next, the separation of REEs from major AMD gangue elements was investigated using synthetic leachate solutions with concentrations similar to those expected from the pre-concentrate samples. This process showed that the grade targets could easily be met when combining optimal parameters from each step. From this primarily work with synthetic solutions, an optimal SX process was developed and validated using a real leachate generated from a pre-concentrate sample. By integrating leachate preparation, solvent extraction, scrubbing, stripping, and oxalic acid precipitation, an oxide containing 90.5% rare earth oxides was generated. The detailed findings are listed as follows:

1) D2EHPA can be used to extract the REEs of Sc(III), Ce(IV), Nd(III), Dy(III) and Y(III) efficiently. The extraction efficiency increases with the increase of aqueous pH and D2EHPA concentration.

2) Elixore range is proven a better choice of diluent than kerosene due to its high performance in the extraction of REEs as well as in the safety evaluation.

3) HCl and HNO_3 can be used to recover Ce(IV), Nd(III), Dy(III) and Y(III) from D2EHPA. Their stripping efficiency in both acids increases with the increase of acid concentration and HCl provides better recovery of REEs.

4) The use of NaOH provides a practical method to recover Sc(III) from D2EHPA by forming $Sc(OH)_3$ precipitate.

5) The addition of TBPO will not only help the extraction of the five REEs but also the phase separation in stripping of Sc(III) with NaOH.

6) The extraction system was determined by using D2EHPA as the extractant, Elixore 205 as the diluent, and TBPO as the modifier. Nearly 100% of the extraction efficiency of the five surrogate REEs were obtained when solvent extraction experiments were conducted with 0.2 M D2EHPA + TBPO in Elixore 205 at pH 2. HCl was selected as the stripping reagent to recover REEs from D2EHPA. 100% of stripping efficiency was obtained for Y(III), Nd(III), Dy(III) and Ce(IV) with 6 M HCl. 75.04% of Sc(III) was recovered from the organic by 2 M NaOH.

7) Reduction of Fe(III) to Fe(II) helps inhibit a large amount of Fe being extracted with REEs. The extraction efficiency of Fe decreases from 97.74% to 6.36% by reduction.

8) D2EHPA is able to selectively extract REEs at low concentrations (100 mg/L) in the presence of a large amount of major gangue elements (>20 g/L).

9) Stripping at low phase ratio (V_A:V_O) will achieve both high recovery of REEs and high retention of gangue metals in the organic phase.

10) Based on the information above, the optimal SX process developed for the recovery of REEs from simulated leachate was determined (Fig 4.10). Through the process, a rare earth oxide with 92.8% purity were obtained.

11) From the validation tests, a laboratory-scale processing flowsheet was developed by integrating leachate preparation, solvent extraction, scrubbing, stripping, and oxalic acid precipitation (Fig 5.7). An oxide containing 90.5% rare earth oxides was generated from a real AMD pre-concentrate sample.

The research demonstrated the technical viability of recovering high purity MREO from AMD pre-concentrate. However, further work is required to develop it to a pilot scale and eventually to an industrial scale. The following lists the work required to achieve this objective.

1) The recycling of the organic phase is critical step in the SX process. Further study need to performed on the stripping stage to ensure effective removal of metals from loaded organic and the subsequent reuse of the organic.

2) This processing flowsheet was developed at a laboratory-scale. Further work need to be done to test the process at a pilot-scale.

3) The commercial realization of this process will be assisted by its integration with a pre-concentrate process that produces high-quality precipitate from AMD, as well as further downstream processing of the mixed REE oxide into individual REE oxide.

Reference

Akabzaa, T., Armah, T., & Baneong-Yakubo, B. (2007). Prediction of acid mine drainage generation potential in selected mines in the Ashanti Metallogenic Belt using static geochemical methods. *Environmental Geology, 52*(5), 957-964.

Akcil, A., & Koldas, S. (2006). Acid Mine Drainage (AMD): causes, treatment and case studies. *Journal of Cleaner Production, 14*(12-13), 1139-1145.

Al-Thyabat, S., & Zhang, P. (2015). In-line extraction of REE from Dihydrate (DH) and HemiDihydrate (HDH) wet processes. *Hydrometallurgy, 153*, 30-37.

Ali, S. (2014). Social and environmental impact of the rare earth industries. *Resources, 3*(1), 123-134.

Allaedini, G., & Zhang, P. (2019). Treatment of phosphoric acid sludge for rare earths recovery II: effect of sonication and flocculant solution temperature on settling rate. *Separation Science and Technology, 54*(11), 1842-1852.

Battsengel, A., Batnasan, A., Haga, K., & Shibayama, A. (2018). Selective separation of light and heavy rare earth elements from the pregnant leach solution of apatite ore with D2EHPA. *Journal of Minerals and Materials Characterization and Engineering, 6*(05), 517.

Bau, M. (1996). Controls on the fractionation of isovalent trace elements in magmatic and aqueous systems: evidence from Y/Ho, Zr/Hf, and lanthanide tetrad effect. *Contributions to Mineralogy and Petrology, 123*(3), 323-333.

Binnemans, K., & Jones, P. T. (2014). Perspectives for the recovery of rare earths from end-of-life fluorescent lamps. *Journal of Rare Earths, 32*(3), 195-200.

Binnemans, K., Jones, P. T., Blanpain, B., Van Gerven, T., & Pontikes, Y. (2015). Towards zero-waste valorisation of rare-earth-containing industrial process residues: a critical review. *Journal of Cleaner Production, 99*, 17-38.

Blowes, D., Ptacek, C., Jambor, J., & Weisener, C. (2003). The geochemistry of acid mine drainage. *Treatise on geochemistry, 9*, 612.

Borra, C. R., Blanpain, B., Pontikes, Y., Binnemans, K., & Van Gerven, T. (2016). Recovery of rare earths and other valuable metals from bauxite residue (red mud): a review. *Journal of Sustainable Metallurgy, 2*(4), 365-386.

Brake, S., Connors, K., & Romberger, S. (2001). A river runs through it: impact of acid mine drainage on the geochemistry of West Little Sugar Creek pre-and post-reclamation at the Green Valley coal mine, Indiana, USA. *Environmental Geology, 40*(11-12), 1471-1481.

Chakhmouradian, A. R., & Wall, F. (2012). Rare earth elements: minerals, mines, magnets (and more). *Elements, 8*(5), 333-340.

Chapman, B., Jones, D., & Jung, R. F. (1983). Processes controlling metal ion attenuation in acid mine drainage streams. *Geochimica et Cosmochimica Acta, 47*(11), 1957-1973.

Chiou, M.-S., & Li, H.-Y. (2002). Equilibrium and kinetic modeling of adsorption of reactive dye on cross-linked chitosan beads. *Journal of hazardous materials, 93*(2), 233-248.

Chu, S. (2011). Department of Energy "Critical Materials Strategy": December.

Da Silva, E. F., Bobos, I., Matos, J. X., Patinha, C., Reis, A., & Fonseca, E. C. (2009). Mineralogy and geochemistry of trace metals and REE in volcanic massive sulfide host rocks, stream sediments, stream waters and acid mine drainage from the Lousal mine area (Iberian Pyrite Belt, Portugal). *Applied Geochemistry, 24*(3), 383-401.

Dutta, Tanushree, et al. "Global demand for rare earth resources and strategies for green mining." Environmental Research 150 (2016): 182-190.El-Didamony, H., Ali, M., Awwad, N., Fawzy, M., & Attallah, M. (2011). Treatment of phosphogypsum waste using suitable organic extractants. *Journal of radioanalytical and nuclear chemistry, 291*(3), 907-914.

El-Yamani, I., & Shabana, E. (1985). Solvent extraction of lanthanum (III) from sulphuric acid solutions by Primene JMT. *Journal of the Less Common Metals, 105*(2), 255-261.

Ferron, C. J., Bulatovic, S. M., & Salter, R. S. (1991). *Beneficiation of rare earth oxide minerals.* Paper presented at the Materials Science Forum.

Foos, A. (1997). Geochemical modeling of coal mine drainage, Summit County, Ohio. *Environmental Geology, 31*(3-4), 205-210.

Free, M. L. (2013). *Hydrometallurgy: fundamentals and applications*: John Wiley & Sons.

Graedel, T., Allwood, J., Birat, J., Reck, B., Sibley, S., Sonnemann, G., . . . Hagelüken, C. (2011). UNEP (2011) Recycling Rates of Metals-A Status Report, A Report of the Working Group on the Global Metal Flows to the International Resource Panel. *International Resource Panel, WGotGMF (Ed.) United Nations Environment Programme*.

Grawunder, A., Merten, D., & Büchel, G. (2014). Origin of middle rare earth element enrichment in acid mine drainage-impacted areas. *Environmental Science and Pollution Research, 21*(11), 6812-6823.

Habashi, F. (1985). The recovery of the lanthanides from phosphate rock. *Journal of Chemical Technology and Biotechnology. Chemical Technology, 35*(1), 5-14.

Hatch, G. P. (2012). Dynamics in the global market for rare earths. *Elements, 8*(5), 341-346.

Hedin, R. S. (2006). The use of measured and calculated acidity values to improve the quality of mine drainage datasets. *Mine Water and the Environment, 25*(3), 146-152.

Huang, X.-Y., Bin, J.-P., Bu, H.-T., Jiang, G.-B., & Zeng, M.-H. (2011). Removal of anionic dye eosin Y from aqueous solution using ethylenediamine modified chitosan. *Carbohydrate Polymers, 84*(4), 1350-1356.

Ismail, N. A., Aziz, M. A. A., Yunus, M. Y. M., & Hisyam, A. Selection of Extractant in Rare Earth Solvent Extraction System: A Review.

Itoh, M., Miura, K., & Machida, K.-i. (2009). Novel rare earth recovery process on Nd–Fe–B magnet scrap by selective chlorination using NH4Cl. *Journal of Alloys and Compounds, 477*(1-2), 484-487.

Jha, M. K., Kumari, A., Panda, R., Kumar, J. R., Yoo, K., & Lee, J. Y. (2016). Review on hydrometallurgical recovery of rare earth metals. *Hydrometallurgy, 165*, 2-26.

Johnson, C. A. (1986). The regulation of trace element concentrations in river and estuarine waters contaminated with acid mine drainage: The adsorption of Cu and Zn on amorphous Fe oxyhydroxides. *Geochimica et Cosmochimica Acta, 50*(11), 2433-2438.

Johnson, D. B., & Hallberg, K. B. (2005). Acid mine drainage remediation options: a review. *Science of the total environment, 338*(1-2), 3-14.

Jordens, A., Cheng, Y. P., & Waters, K. E. (2013). A review of the beneficiation of rare earth element bearing minerals. *Minerals Engineering, 41*, 97-114.

Josso, P., Roberts, S., Teagle, D. A., Pourret, O., Herrington, R., & de Leon Albarran, C. P. (2018). Extraction and separation of rare earth elements from hydrothermal metalliferous sediments. *Minerals Engineering, 118*, 106-121.

Jung, H.-B., Yun, S.-T., Mayer, B., Kim, S.-O., Park, S.-S., & Lee, P.-K. (2005). Transport and sediment–water partitioning of trace metals in acid mine drainage: an example from the abandoned Kwangyang Au–Ag mine area, South Korea. *Environmental Geology, 48*(4-5), 437-449.

Kelly, E., & Spottiswood, D. (1989). The theory of electrostatic separations: A review Part I. Fundamentals. *Minerals Engineering, 2*(1), 33-46.

Kijkowska, R., Kowalczyk, J., Mazanek, C., Mikolajczyk, T., & Pawlonska-Kozinska, D. (1989). Rare earth elements from Kola apatite phosphogypsum. *Phosphorus and potassium*(163), 22-26.

Koopman, C., & Witkamp, G. (2000). Extraction of lanthanides from the phosphoric acid production process to gain a purified gypsum and a valuable lanthanide by-product. *Hydrometallurgy, 58*(1), 51-60.

Krishnamurthy, N., & Gupta, C. K. (2004). *Extractive metallurgy of rare earths*: CRC press.

Li, H. (2010). Recovery of rare earths from phosphor sludge by acid leaching. *Chinese Journal of Rare Metals, 34*(6), 899-904.

Li, X., Wei, C., Deng, Z., Li, M., Li, C., & Fan, G. (2011). Selective solvent extraction of vanadium over iron from a stone coal/black shale acid leach solution by D2EHPA/TBP. *Hydrometallurgy, 105*(3-4), 359-363.

Liu, Y., & Naidu, R. (2014). Hidden values in bauxite residue (red mud): Recovery of metals. *Waste management, 34*(12), 2662-2673.

Long, K. R., Van Gosen, B. S., Foley, N. K., & Cordier, D. (2012). The principal rare earth elements deposits of the United States: a summary of domestic deposits and a global perspective *Non-Renewable Resource Issues* (pp. 131-155): Springer.

Massari, S., & Ruberti, M. (2013). Rare earth elements as critical raw materials: Focus on international markets and future strategies. *Resources Policy, 38*(1), 36-43.

McCarthy, T. S. (2011). The impact of acid mine drainage in South Africa. *South African Journal of Science, 107*(5-6), 01-07.

Miekeley, N., de Jesus, H. C., da Silveira, C. P., Linsalata, P., & Morse, R. (1992). Rare-earth elements in groundwaters from the Osamu Utsumi mine and Morro do Ferro analogue study sites, Poços de Caldas, Brazil. *Journal of Geochemical Exploration, 45*(1-3), 365-387.

"National Minerals Information Center." Rare Earths Statistics and Information (2019), www.usgs.gov/centers/nmic/rare-earths-statistics-and-information.

Noack, C. W. (2015). *Measurement and Recovery of Rare Earth Elements from Hypersaline Fluids.* figshare.

Noack, C. W., Dzombak, D. A., & Karamalidis, A. K. (2014). Rare earth element distributions and trends in natural waters with a focus on groundwater. *Environmental science & technology, 48*(8), 4317-4326.

Ochsenkühn-Petropoulou, M. T., Hatzilyberis, K. S., Mendrinos, L. N., & Salmas, C. E. (2002). Pilot-plant investigation of the leaching process for the recovery of scandium from red mud. *Industrial & engineering chemistry research, 41*(23), 5794-5801.

Onghena, B. (2018). Ionic liquid solvent extraction for the recovery of rare earths and cobalt.

Parhi, P., Park, K., Nam, C., & Park, J. (2015). Liquid-liquid extraction and separation of total rare earth (RE) metals from polymetallic manganese nodule leaching solution. *Journal of Rare Earths, 33*(2), 207-213.

Peelman, S., Sun, Z. H., Sietsma, J., & Yang, Y. (2016). Leaching of rare earth elements: review of past and present technologies *Rare Earths Industry* (pp. 319-334): Elsevier.

Peppard, D., Mason, G., Driscoll, W., & Sironen, R. (1958). Acidic esters of orthophosphoric acid as selective extractants for metallic cations—tracer studies. *Journal of Inorganic and Nuclear Chemistry, 7*(3), 276-285.

Pereira, F., & Bilal, E. (2012). Phosphoric acid extraction and rare earth recovery from apatites of the Brazilian phosphatic ores.

Pérez-López, R., Delgado, J., Nieto, J. M., & Márquez-García, B. (2010). Rare earth element geochemistry of sulphide weathering in the São Domingos mine area (Iberian Pyrite Belt): a proxy for fluid–rock interaction and ancient mining pollution. *Chemical Geology, 276*(1-2), 29-40.

Pietrelli, L., Bellomo, B., Fontana, D., & Montereali, M. (2002). Rare earths recovery from NiMH spent batteries. *Hydrometallurgy, 66*(1-3), 135-139.

Podbiera-Matysik, K., Gorazda, K., & Wzorek, Z. (2015). Potencial management of waste phosphogypsum with particular focus on recovery of rare earth metals. *Polish Journal of Chemical Technology, 17*(1), 55-61.

Preston, J. (1996). The recovery of rare earth oxides from a phosphoric acid byproduct. Part 4. The preparation of magnet-grade neodymium oxide from the light rare earth fraction. *Hydrometallurgy, 42*(2), 151-167.

Preston, J., Cole, P., Craig, W., & Feather, A. (1996). The recovery of rare earth oxides from a phosphoric acid by-product. Part 1: Leaching of rare earth values and recovery of a mixed rare earth oxide by solvent extraction. *Hydrometallurgy, 41*(1), 1-19.

Preston, J., Cole, P., Du Preez, A., Fox, M., & Fleming, A. (1996). The recovery of rare earth oxides from a phosphoric acid by-product. Part 2: The preparation of high-purity cerium dioxide and recovery of a heavy rare earth oxide concentrate. *Hydrometallurgy, 41*(1), 21-44.

Preston, J., Du Preez, A., Cole, P., & Fox, M. (1996). The recovery of rare earth oxides from a phosphoric acid by-product. Part 3. The separation of the middle and light rare earth fractions and the preparation of pure europium oxide. *Hydrometallurgy, 42*(2), 131-149.

Preston, J. S., & Du Preez, A. C. (1998). The recovery of a mixed rare-earth oxide and the preparation of cerium, europium and neodymium oxides from a South African phosphoric acid sludge by solvent extraction. *Mineral Processing and Extractive Metullargy Review, 18*(2), 175-200.

Rabatho, J. P., Tongamp, W., Takasaki, Y., Haga, K., & Shibayama, A. (2013). Recovery of Nd and Dy from rare earth magnetic waste sludge by hydrometallurgical process. *Journal of Material Cycles and Waste Management, 15*(2), 171-178.

Reddy, M., Prasada Rao, T., & Damodaran, A. (1993). Liquid-liquid extraction processes for the separation and purification of rare earths. *Mineral Procesing and Extractive Metallurgy Review, 12*(2-4), 91-113.

Sahoo, P., Tripathy, S., Equeenuddin, S. M., & Panigrahi, M. (2012). Geochemical characteristics of coal mine discharge vis-à-vis behavior of rare earth elements at Jaintia Hills coalfield, northeastern India. *Journal of Geochemical Exploration, 112*, 235-243.

Schemel, L. E., Kimball, B. A., & Bencala, K. E. (2000). Colloid formation and metal transport through two mixing zones affected by acid mine drainage near Silverton, Colorado. *Applied Geochemistry, 15*(7), 1003-1018.

Skousen, J.G. and P.F. Ziemkiewicz (1996). Acid mine drainage control and treatment. Morgantown, WV: West Virginia University and the National Mine Land Reclamation Center.

Seredin, V. V., & Dai, S. (2012). Coal deposits as potential alternative sources for lanthanides and yttrium. *International Journal of Coal Geology, 94*, 67-93.

Soltani, N., Moore, F., Keshavarzi, B., & Sharifi, R. (2014). Geochemistry of trace metals and rare earth elements in stream water, stream sediments and acid mine drainage from Darrehzar Copper Mine, Kerman, Iran. *Water Quality, Exposure and Health, 6*(3), 97-114.

Sprecher, B., Xiao, Y., Walton, A., Speight, J., Harris, R., Kleijn, R., . . . Kramer, G. J. (2014). Life cycle inventory of the production of rare earths and the subsequent production of NdFeB rare earth permanent magnets. *Environmental science & technology*, *48*(7), 3951-3958.

Stewart, B. W., Capo, R. C., Hedin, B. C., & Hedin, R. S. (2017). Rare earth element resources in coal mine drainage and treatment precipitates in the Appalachian Basin, USA. *International Journal of Coal Geology, 169*, 28-39.

Sun, H., Zhao, F., Zhang, M., & Li, J. (2012). Behavior of rare earth elements in acid coal mine drainage in Shanxi Province, China. *Environmental earth sciences, 67*(1), 205-213.

Sun, X., Zhao, J., Meng, S., & Li, D. (2005). Synergistic extraction and separation of yttrium from heavy rare earths using mixture of sec-octylphenoxy acetic acid and bis (2, 4, 4-trimethylpentyl) phosphinic acid. *Analytica Chimica Acta, 533*(1), 83-88.

US EPA (1994). Technical Document: Acid Mine Drainage Prediction. December. Washington DC: U.S. Environmental Protection Agency.

Vass, C. R. (2019). A Critical Assessment on the Resources and Extraction of Rare Earth Elements from Acid Mine Drainage.

Vass, C. R., Noble, A., & Ziemkiewicz, P. F. (2019). The Occurrence and Concentration of Rare Earth Elements in Acid Mine Drainage and Treatment By-products: Part 1—Initial Survey of the Northern Appalachian Coal Basin. *Mining, Metallurgy & Exploration*, 1-14.

Walawalkar, M. (2016). *Extraction of Rare Earth Elements from Phosphogypsum (Fertilizer Production By-product).*

Wang, W., Pranolo, Y., & Cheng, C. Y. (2013). Recovery of scandium from synthetic red mud leach solutions by solvent extraction with D2EHPA. *Separation and Purification Technology, 108*, 96-102.

Wei, X., Viadero Jr, R. C., & Buzby, K. M. (2005). Recovery of iron and aluminum from acid mine drainage by selective precipitation. *Environmental Engineering Science*, *22*(6), 745-755.

Wilson, A. M., Bailey, P. J., Tasker, P. A., Turkington, J. R., Grant, R. A., & Love, J. B. (2014). Solvent extraction: the coordination chemistry behind extractive metallurgy. *Chemical society reviews, 43*(1), 123-134.

Wu, S., Wang, L., Zhao, L., Zhang, P., El-Shall, H., Moudgil, B., . . . Zhang, L. (2018). Recovery of rare earth elements from phosphate rock by hydrometallurgical processes–A critical review. *Chemical Engineering Journal, 335*, 774-800.

Xie, F., Zhang, T. A., Dreisinger, D., & Doyle, F. (2014). A critical review on solvent extraction of rare earths from aqueous solutions. *Minerals Engineering, 56*, 10-28.

Yang, F., Kubota, F., Baba, Y., Kamiya, N., & Goto, M. (2013). Selective extraction and recovery of rare earth metals from phosphor powders in waste fluorescent lamps using an ionic liquid system. *Journal of hazardous materials, 254*, 79-88.

Zaimes, G. G., Hubler, B. J., Wang, S., & Khanna, V. (2015). Environmental life cycle perspective on rare earth oxide production. *ACS Sustainable Chemistry & Engineering, 3*(2), 237-244.

Zhang, J., & Edwards, C. (2012). *A review of rare earth mineral processing technology.* Paper presented at the 44th Annual Meeting of the Canadian Mineral Processors. CIM, Ottawa.

Zhang, J., Zhao, B., & Schreiner, B. (2016). *Separation hydrometallurgy of rare earth elements*: Springer.

Zhao, F., Cong, Z., Sun, H., & Ren, D. (2007). The geochemistry of rare earth elements (REE) in acid mine drainage from the Sitai coal mine, Shanxi Province, North China. *International Journal of Coal Geology, 70*(1-3), 184-192.

Zielinski, S., Szczepanik, A., Buca, M., & Kunecki, M. (1993). Recovery of lanthanides from Kola apatite in phosphoric acid manufacture. *Journal of Chemical Technology & Biotechnology, 56*(4), 355-360.

Ziemkiewicz, P., He, T., Noble, A., & Liu, X. (2016). Recovery of rare earth elements (REEs) from coal mine drainage. *US Department of Energy, National Energy Technology Laboratory*.